Pathophysiological roles of mast cell in brain ischemic models of mice

（マウス脳虚血モデルにおけるマスト細胞の役割）

Mutsuki KURAOKA

倉岡　睦季

担当教員　吉川　泰弘　Yasuhiro YOSHIKAWA

TABLE OF CONTENTS

General Introduction

Ischemic brain damage, or brain-stroke (brain infarct), is of great importance in the morbidity of older people. It is now being the third most common cause of death after cancer and heart disease in the developed countries. The aging (senility) is a major risk factor for ischemic stroke; the prevalence rises exponentially from the age of 55 years, and correlates with the increase in all types of cerebrovascular pathology [Posner et al., 1984]. Since survived many patients are suffered from limitation of quality of life by their neurological sequelae, the financial and social impact of stroke-related disorders cannot be understated.

Ischemic stroke is a complex of neurological disorders characterized by loss of cerebral blood flow, significant cell death with both necrotic and apoptotic in nature, edematous swelling, and an enhanced inflammatory response in the brain [Dirnagl et al., 1999]. Many mechanisms, however, have not yet been cleared. To define pathophysiological mechanisms and therapeutic treatments, it is necessary for equipment of useful ischemic models such as gene-manipulated experimental animals. Especially, murine ischemic models have attracted an increasing attention, because of the abundant availability of genetically altered (transgenic or knockout and mutant) strains [Chan, 1998].

Experimental ischemic models are generally divided into the two types: focal and global ischemic models [Small et al., 1999]. In focal model, infarct lesion is characterized with a necrotic core, salvageable penumbra and normal tissue similarly to those of human stroke. On the other hand, global ischemia induces delayed and selective neuronal death (e.g. CA1 region of the hippocampus) or cellular damage in robust areas of hemispheres, corresponding to the duration time of ischemia [Small and Buchan, 2000]. Both focal and global ischemic models in

mice are applied to various studies, supposing the ischemic region, severity and therapeutic targets.

In the present study, I firstly analyzed efficient induction of focal brain ischemia in mice (Chapter 1). Because it is an important problem that variation of infarct-sizes frequently occurs after an experimental artery occlusion. Secondly, I studied the mast cell-related pathophysiological mechanisms using murine focal and global ischemic models (Chapter 2&3). Recently, mast cells are recognized as an important trigger of edematous and inflammatory mechanisms. Many functions of mast cell are reported in various diseases, but little is cleared in brain ischemia. In Chapter 2, an expansion of infarct lesion was analyzed in murine focal models, which were treated with mast cell-modulation agents or originally deficient for mast cell. In Chapter 3, I studied global ischemic lesions of mast cell-deficient mouse, remarkably expression of matrix metalloproteinase (MMP) that exacerbates ischemic damages. In general introduction, I summarized the overview of the pathophysiology of ischemic stroke, mast cell and MMPs as follows.

Pathophysiology of ischemic stroke

Subtypes of stroke: Stroke is classified into two general types which are ischemic stroke and hemorrhagic stroke. In the ischemic stroke, decreased or absent blood circulation result from blood-flow obstructions deprives neurons as well as neuronal functions. Intracerebral hemorrhage, often occurs as a result of hypertension, originates from deep penetrating vessels and causes injury to brain tissue by disrupting connecting blood pathways and causing localized pressure injuries. In either case, destructive biochemical substances released from a variety of sources

play an important role in tissue damage and destruction.

Ischemic stroke is commonly considered nevertheless its origin as atherothrombotic, cardioembolic or lacunar [National Institute of Neurological Disorders and Stroke *ad Hoc* Committee in USA, 1990]. Atherothrombotic stroke occurs with atherosclerosis involving selected sites in the extracranial and major intracranial arteries. Cardioembolic stroke occurs after cardiac thrombi lodge in the cerebral arterial tree. Lacunar stroke occurs in patients with nonatherothrombotic obstruction of the small (< 1.5 cm), perforating arteries that supply blood to the deep cortical structures (a process called lopohyalinosis).

Mechanisms for death of neural cells: Brain metabolism is steady and continuous with no resting period, which requires a continuous supply of oxygen and glucose. It is highly dependent upon oxygen and accounts for 20% of the body's oxygen usage. Thus, the reduction of blood flow even a few minutes may cause irreversible neuronal damage [Frosch et al., 2005]. Sustained hypoglycemia may also damage brain tissue, due to glucose being the major energy source in the brain. Since neurons do not store glycogen, energy depletion is quite rapidly occurred when blood flow is decreased.

The mechanisms of neuronal cell death have not been fully defined and the relative contribution of apoptotic and necrotic processes remains controversial. Necrotic cell death is characterized by cell swelling, membrane disruption, and random DNA breaks, whereas apoptotic cell death involves chromatin condensation, internucleosomal DNA fragmentation, blebbing of the plasma membrane, and the appearance of apoptotic bodies [Small et al., 1999]. Rapid neuronal death after

ischemia, such as occurs in the ischemic core, is necrotic, whereas delayed neuronal cell death in the penumbral region may be apoptotic. And it is discussed that molecular-biological and biochemical mixing processes are involved along the apoptosis-necrosis continuum [Martin et al., 1998].

The signaling pathways can initiate the cascade events that lead to the death of the neuron during ischemia. Cell surface signaling events include the activities of both voltage- and ligand-gated ion channels including K^+, Na^+, Ca^{2+} channels, ionotropic and metabotropic glutamate and gamma-aminobutyric acid (GABA) receptors, and adenosine receptors. All of these cell surface molecules may contribute to the pathophysiology of ischemic cell death [Small et al., 1999].

Animal models: As tools to help better understanding the pathophysiological mechanisms underlying stroke in man, animal models of brain stroke have been developed that can be grouped into 2 main types; global and focal ischemia [Small et al., 1999]. In the case of global ischemic models, the lack of blood flow should be transient (5-30 min), because complete or nearly complete destruction of neural tissues occurred (remaining <5% of normal tissues in the cortex) during this time. If blood flow is not restored for long time, widespread pan-necrosis ensues and there is no functional recovery of the brain tissues. After reperfusion within short time, there is selective neuronal death of pyramidal neurons in the CA1 region of the hippocampus and in layers 3, 5 and 6 on the neocortex as well as cerebellar Purkinje neurons and medium-sized striatal neurons. The sensitivity of these neurons to ischemia differs between brain regions as does the time course of cell death. This model most closely represents the clinical situation of a cardiac arrest or near

drowning. Bilateral common carotid artery occlusion (CCAO) is performed to induce global cerebral ischemia.

The focal occlusion models are a closer representation of the clinical situation in which there is a localized, more prolonged (60-90 min) ischemic period resulting from the occlusion of an individual cerebral vessels. The resulting blood flow pattern is more complex and is not as severe as in the global ischemic models. There is a central core region, closest to the occluded vessel, which results in immediate pan-necrosis, if reperfusion is not reestablished within 60 min of the occlusion. Surrounding the edge of the core lesion is a region referred to as the penumbra, which is hypoperfused and is at risk of dying but can be salvaged with increased perfusion and/or pharmacological intervention. To make focal models, middle cerebral artery occlusion (MCAO) is transiently or permanently performed. The MCAO model has mainly been induced by either direct or indirect approach methods. The direct MCAO method is performed with the microsurgical techniques of coagulation [Yamamoto et al., 1988; Hatashita and Hoff, 1990; Kanemitsu et al., 2002] or ligation [Coyle, 1982; Chen et al., 1986; Xi et al., 2004] on the distal middle cerebral artery (MCA). The potential for invasion might increase in brain tissue, because craniectomy is also necessary for this method. On the other hand, the indirect MCAO method occludes the origin of MCA intraluminally with a monofilament thread through the unilateral common carotid artery (CCA) [Belayev et al., 1999; Clark et al., 1997; Takano et al., 1997; Kitagawa et al., 1998; Wexler et al., 2002; Tsuchiya et al., 2003]. The intraluminal thread model has the benefit of no brain invasion, so that a large number of studies have been performed under these conditions.

Inflammatory and glial response: Inflammatory response to tissue injury is initiated by the rapid production of many different inflammatory mediators such as tumor necrosis factor (TNF)-α and prostaglandin E2. Leukocyte recruitment to ischemic areas occurs as early as thirty minutes after ischemia and reperfusion. Accumulated leukocytes mechanically obstruct blood flow and worsen cerebral microcirculation (no-reflow phenomenon). Leukocytes also activate vasoactive substances such as oxygen free radicals, arachidonic acid metabolites, cytokines and nitric acid. These mediators bring about vasodilation, vasoconstriction, increased permeability and platelet and leukocyte adherence to the endothelial wall.

Endothelial cells are one of the first cell types to respond to hypoxia. This response occurs at morphological and biochemical levels. Morphologically, endothelial cells swell and form "microvilli" at the luminal surface of the cell. This results in a reduction in the luminal patency of the capillary vessel. Mechanical plugging by erythrocytes, leukocytes and platelets follows. At a biochemical level, endothelial cells mediate the effects of vasoactive agents such as endothelin peptides, eicosanoids, and smooth muscle relaxant (probably nitric acid), which in part modulate the vascular tone of the microcirculation. Activation of endothelial adhesion molecules promotes leukocyte adherence to the endothelial wall, a key process in initiation of the inflammatory process.

Brain injury (e.g. ATP release) triggers rapid activation of microglial cells. When neuronal cells die, microglia can be further activated and become phagocytes for clearance of cellular debris. These activated microglias participate in the pathogenesis of brain ischemia by secreting various inflammatory molecules such as cytokines and prostaglandins that signal to astrocytes amplifying their

inflammatory response and resulting in even more injurious accumulation of neurotoxins in brain tissue. Microglia activation also results in the release of chemotactic factors that recruit more microglia to the site of activation as well as promote the infiltration of immune-cells from the peripheral blood [Garden and Möller, 2006].

Many functions of astrocytes are likely to be important in determining the tissue response to ischemia, including their role in the control of fluid movements between the intracellular and extracellular space, the ability to take up glutamate and reduce excitotoxicity, and the role in spatial buffering. Astrocytes also play a crucial part in the antioxidant defense of the brain, containing the highest concentrations of antioxidants as well as providing the neurons with substrates for antioxidants such as glutathione. However, in an excitatory crisis, the potentially protective functions of reactive astrocytes can eventually be reduced or even reversed and might instead contribute to the development of neural damage. Thus, activated astrocytes might both protect from and contribute to the glutamate-mediated neuronal damage. At the chronic stage of ischemia, upregulation of intermediate filament proteins, particular glial fibrillary acidic protein (GFAP) and cellular hypertrophy are observed as hallmark of “reactive astrocytosis”. Reactive astrocytes migrate over considerable distances to sites of injury, and develop post-ischemic glial scars. The post-ischemic glial scars play a role in healing, such as reconstruction of blood-brain barrier (BBB), neurite outgrowth and regulatory volume decrease in counteracting the development of brain edema [Pekny and Nilsson, 2005].

Brain swelling and edema: Brain swelling is harmful because of its effects on adjacent tissues and these effects are magnified by the fixed volume of the skull [Simard et al., 2007]. Swollen tissues exert a mechanical force on the surrounding shell of tissue, displacing it and increasing tissue pressure within it. As the intracranial pressure rises maximally at 24-72 h, cerebral perfusion pressure and cerebral blood flow are reduced to the levels that cannot support brain metabolism, and result in "brain death" [Rosenberg, 1999; Ayata and Ropper, 2002].

Hemispheric swelling is caused by brain edema following ischemia-induced cytotoxity and an increase in capillary permeability [Simard et al., 2007]. Movement of water contents and plasma proteins from a capillary into brain tissue is observed concomitant with the loss of autoregulation of the BBB. Many factors including the hydraulic conductivity of capillaries, hydrostatic and osmotic pressure gradients, and tissue compliance and resistance, modify edema formation [Mayhan et al., 2001; Simard et al., 2007]. It is known that some factors, such as histamine, oxygen radicals and cytokines (e.g. TNF-α), influence directly cerebral endothelial cells, and promote capillary permeability [Akassoglou et al., 1997; Rosenberg, 1999; Mayhan et al., 2001; Ayata and Ropper, 2002]. And some proteases (e.g. matrix metalloproteinase, chymase, plasminogen activators) are involved in the breakdown of BBB integrity, and result in increased exudates.

Mast cell

Mast cell function: Mast cells are being recognized as sentinels of innate immunity and modulators of adaptive immunity, through the release of biologically highly active cytokines, chemokines, lipid mediators, proteases and biogenic amines [Heib

et al., 2008]. They are located at strategic site such as skin, and the vascular and mucosal barriers; they bind IgE on their surface by expressing the high affinity Fc receptor for IgE (FcεRI). Similarly, IgE-independent stimuli (e.g. trauma, complements, enzymes, pharmacological agents) potently induce mast cell activation. Because mast cells contain metachromatic granules which consist of substances such as vasoactive, anticoagulant and proteolytic factors, and cytokines [Gordon and Galli, 1991; Holgate, 2000], mast cells can show multi functions as early as degranulation.

Mast cells strongly regulate vosodilation and vascular permeability by selective release of mediators (TNF-α, histamine, bradykinin, leukotriens), so that they have a key role on edema formation. Secretary granules also contain proteolytic enzymes (matrix metalloproteinases, chymase, triptase), and these factors relate with blood vascular disruptions and edema, and tissue breakdown and remodeling. Furthermore, by release of pro-inflammatory cytokines (TNF-α, IL-1, IL-6) and chemokines (NCF, BCF, ECF-A), mast cells activate immune-cells, neutrophils, eosinophils, basophils, monocytes and lymphocytes, and recruit them into the tissue site from the peripheral blood [Heib et al., 2008]. These mechanisms are indicated in a schema (Fig. GI-1).

Brain mast cells: The ubiquity of mast cells in vertebrate brains has been well documented, at the perivascular and intraparenchymal sites of the cortex, hippocampus, thalamus, and hypothalamus (Fig. GI-2) [Grzanna and Shultz, 1982; Russell et al., 1990; Johnson and Krenger, 1992; Hendrix et al., 2006]. Similarly to other organs, brain mast cells regulate vascular permeability and inflammatory

activation by selective release of mediators [Theoharides, 1990; Zhuang et al., 1996].

Furthermore, mast cell-nervous system interactions are observed in normal brains. For example, histamine, serotonin, and 5-HT, which are released by activated mast cells, are a major neurotransmitter. Contrary, the major neuropeptides, such as substance P, calcitonin gene-related peptide (CGRP), vasoactive intestinal polypeptide (VIP), neurokinins, bradykinin, somatostatin, neurotensin, neuropeptide Y, opioid peptide and adenosine nucleotides have been reported to stimulate mast cells. This involvement may be linked to activation of resident mast cells in neurogenic inflammation [Johnson and Krenger, 1992]. And astrocytes also participate in interaction with mast cells, recruiting mast cells into nervous system [Silver et al., 1996].

Matrix Metalloproteinase

Matrix metalloproteinases (MMPs) belong to a rapidly expanding family of enzymes which have been identified to date more than 20 members. They are Zn^{2+}-dependent endopeptidases, including gelatinases, collagenases, stromelysins and membrane-type MMPs [Chandler et al., 1996; Murphy et al., 1999]. The MMPs are expressed as zymogens that are activated upon proteolytic cleavage of a propeptide. The MMPs cleave proteins of extracellular matrix, but also process a number of cell surface proteins such as receptors, pro-inflammatory cytokines and other soluble proteins. The proteolytic activity of MMPs is controlled by the tissue inhibitors of metalloproteinase (TIMPs), a family of secreted multifunctional proteins that comprises four members (TIMP-1 to TIMP-4), with 30-40% sequence similarity each other [Greene et al., 1996; Cunningham et al., 2005]. All TIMPs

inhibit the active forms of most MMPs by forming noncovalent 1:1 complexes with them.

Excessive or inappropriate expression of MMPs can induce pathological processes, and it is well known that alterations in the expression and activity of MMPs are linked to the development of several brain diseases. Recently, neurologists have gained interest in the potential implication of MMPs in the pathophysiology of brain ischemia. The MMP-2 (gelatinase A) and MMP-9 (gelatinase B) are up-regulated in rodent brains after global and focal ischemia [Romanic et al., 1998; Rosenberg et al., 2001; Rivera et al., 2002; Magnoni et al., 2004], in close association with the breakdown of BBB and the neuroinflammatory response [Rosenberg et al., 1998; Cunningham et al., 2005]. Furthermore, MMP-9 gene knockout mice have been shown to reduce the infarct volume and BBB disruption after transient focal ischemia [Asahi et al., 2001]. These evidences suggest that MMPs, in particular gelatinases MMP-2 and -9, might contribute to ischemic damage but little is known about their mechanisms.

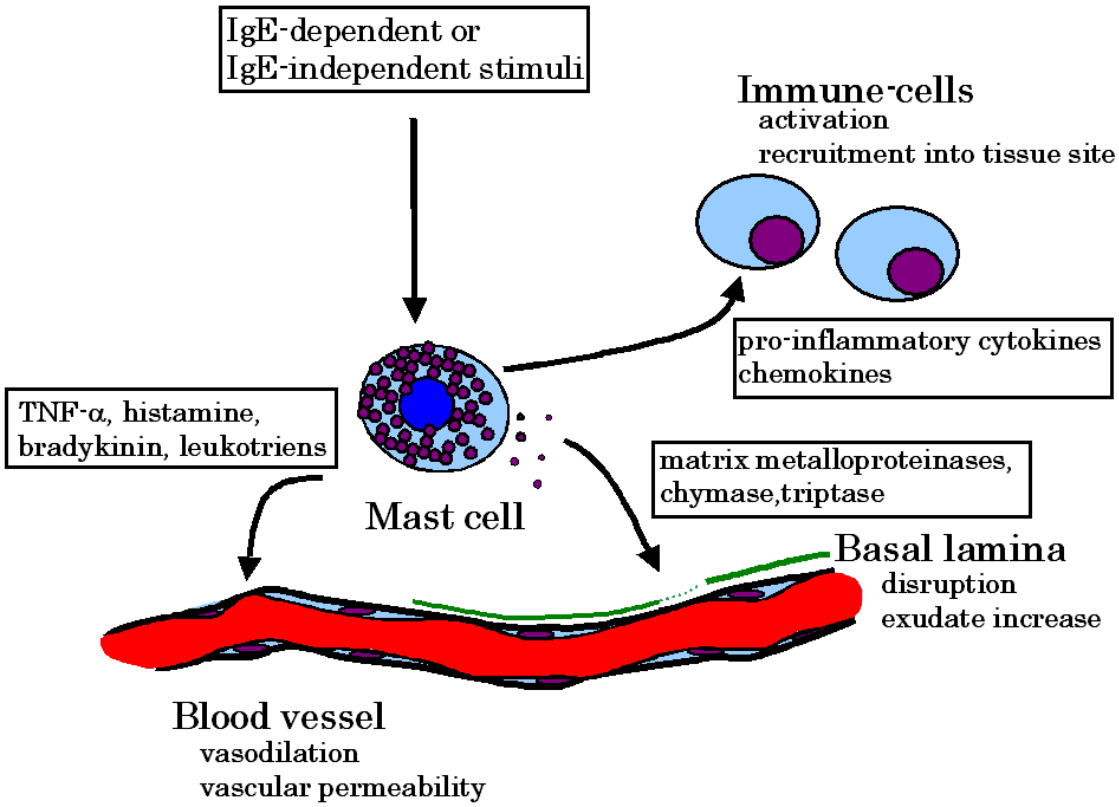

Fig. GI-1

Generic mast cell. This figure shows the potential range of both stimuli and secretary responses of mast cells.

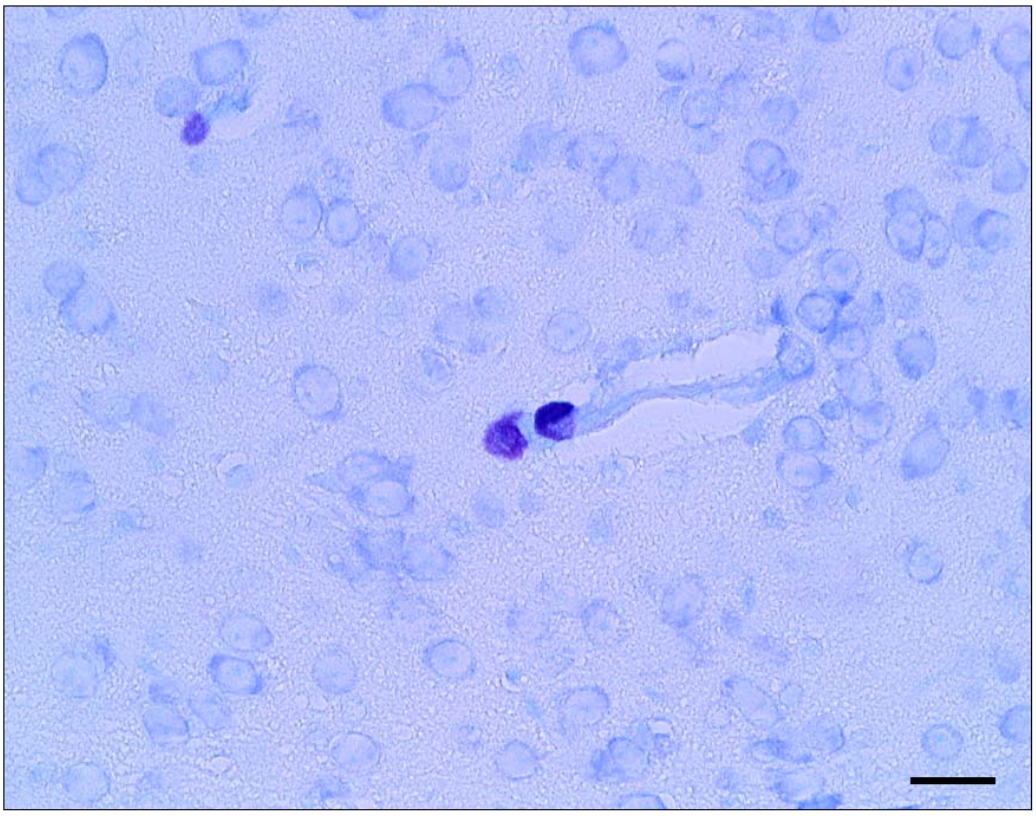

Fig. GI-2

Metachromatic identification of brain mast cells in the thalamus. Note that localization of mast cells around the blood vessel. Toluidine blue staining.

Scale bar: 25 μm.

Chapter 1

Direct experimental occlusion of the distal middle cerebral artery induces high reproducibility of brain ischemia in mice

Abstract

Many investigators have used murine models to investigate the pathophysiology of brain ischemia. A focal ischemic model is a closer approximation to human stroke which includes a necrotic core, penumbra and undamaged tissues. Occlusion of the unilateral artery, especially the middle cerebral artery (MCA), is performed in this model, but collateral circulation often influences a variation of ischemic lesions both qualitatively and quantitatively. It is likely that if the more proximal portion of the artery is unilaterally occluded, the outcomes are the more inconsistent.

The present study was designed to examine the reproducibility of infarct lesion by distal or proximal artery occlusion. Direct occlusion of the distal MCA was performed and compared with unilateral common carotid artery occlusion (CCAO) in C57BL/6 mice. Direct MCA occlusion (MCAO) consistently induced ischemic lesions in cortical areas of the brain. All model animals (n=14) survived 24 h after occlusion, and exhibited a maximum infarct volume (20.0 ± 5.0%). In contrast, permanent and transient unilateral CCAO models had mortality rates of 62.5 and 25.0% at 24h after occlusion, and showed severe to absent lesions with the infarct volumes of 29.0 ± 20.8 and 33.2 ± 24.2%, respectively.

In conclusion, distal MCAO produces high reproducibility of ischemic insults and survivability when compared with unilateral CCAO. Thus, distal MCAO is a useful method for the focal ischemic model using mice.

Introduction

Stroke is one of the most serious human disorders in countries with aging populations. The financial and social impact of stroke-related disorders cannot be understated. Animal models of cerebral infarction are crucial for understanding the mechanisms of neuronal death or survival following ischemic brain injury and for the development of therapeutic interventions for victims of all types of stroke. Many different species, especially rodents, and protocols have been used to obtain further knowledge in this research area.

To induce hemispheric ischemia, occlusion of cerebral arteries distally straight from common carotid arteries (CCAs) has been performed in rodents [Small and Buchan, 2000]. According to the location of arterial occlusion, either global or focal ischemic models are produced. Bilateral CCAs branch in the rostrum area into the internal carotid arteries (ICAs) and external carotid arteries (ECAs). And bilateral ICAs link basilar arteries and form the Circle of Willis at the cerebral base [Ward et al., 1990]. The Circle of Willis has a connection to cerebral arteries, such as the anterior cerebral artery (ACA), middle cerebral artery (MCA) and posterior cerebral artery (PCA). These arteries supply blood to each cerebral region. Bilateral CCA occlusion (CCAO) has been performed to induce global cerebral ischemia by reducing the blood flow in the Circle of Willis, whereas unilateral MCA occlusion (MCAO) induces focal ischemia [Tamaki et al., 2006].

The focal ischemic model is a closer approximation to human stroke and produces heterogenous pathological lesions which include a necrotic core and salvageable penumbra, as well as normal, undamaged tissue in both the ipsilateral

and contralateral hemispheres [Small and Buchan, 2000]. Unilateral MCAO induces focal lesions in the cortex and caudate putamen, which are limited to MCA territory [Kanemitsu et al., 2002]. Recently, the MCAO model has mainly been induced by direct or indirect approach methods.

Direct MCAO is performed with the microsurgical techniques of coagulation [Yamamoto et al., 1988; Hatashita and Hoff, 1990; Kanemitsu et al., 2002] or ligation [Coyle, 1982; Chen et al., 1986; Xi et al., 2004] on the distal MCA. The potential for invasion might increase in brain tissue, because craniectomy is also necessary for this method. There are only a small number of reports of the craniectomized model in mice, because the operation is considered to be technically difficult [Ohtaki et al., 2005]. On the other hand, the indirect MCAO method occludes the origin of MCA intraluminally with a monofilament thread through the unilateral CCA [Belayev et al., 1999; Clark et al., 1997; Takano et al., 1997; Kitagawa et al., 1998; Wexler et al., 2002; Tsuchiya et al., 2003]. The intraluminal thread model has the benefit of no brain invasion, so that a large number of studies have been performed under these conditions. In a previous study of direct or indirect MCAO rat models, however, the intraluminal thread method was proposed as approximating an ICA occlusion (ICAO) model rather than a simple MCAO model, because indirect MCAO induces ischemic insults outside MCA territory [Kanemitsu et al., 2002]. In C57BL/6 mice, the intraluminal thread model occluded not only MCA but also PCA, and caused severe hemispheric ischemia [Kitagawa et al., 1998]. Thus, direct MCAO may be better than indirect MCAO to get a reproducible focal ischemia within MCA territory in mice models.

On unilateral artery occlusion, the effect of collateral circulation is

indicated as the leading cause of variation of ischemic lesions [Kitagawa et al., 1998; Maeda et al., 1998; 1999]. The cerebral vascular anatomical issues have an advantage in the mouse model because of the availability of strain-specific information. Development of posterior communicating arteries (PcomAs) leads to the lack of uniform architecture in the Circle of Willis [Ozdemir et al., 1999; Kelly et al., 2001] and interferes with ischemic insults in the ipsilateral hemisphere. It is likely that if the more proximal portion of the artery is unilaterally occluded, the outcomes are the more inconsistent.

The present study is designed to examine the induction of infarct lesion by distal and proximal artery occlusion. Direct occlusion of the distal MCA was performed in C57BL/6 mice and was characterized by ischemic insults, involving neuronal death, reaction of glial cells and blood-brain barrier (BBB) damage. I compared the lesions of direct MCAO with unilateral CCAO models involving occlusion of a proximal artery. I also demonstrate the efficiency of unilateral artery occlusion through the ischemic outcomes of distal and proximal artery occlusion.

Materials and Methods

Animals

Specific pathogen-free (SPF) male C57BL/6 mice were purchased from Japan SLC, Inc (Shizuoka, Japan). They were acclimated for 1-2 weeks in a group of 3-4 individuals per a plastic cage (30 × 20 × 13 cm) filled with bedding of flaky spruce material (White Flake; Charles River Laboratories Japan Inc, Kanagawa, Japan). The mice were used at 10-13 weeks of age at weights of 25-30 g. All animals were housed on a 12 h light / dark cycle at a temperature of 22-24 °C and humidity of 40-50%. They were fed on commercial pellets, (MF; Oriental Yeast Co., LTD, Tokyo, Japan) and tap water *ad libitum*. The number of animals used in this study was 78. All animal care and experimentation were conducted in accordance with the guidelines of The University of Tokyo. All the experiments are conducted with an accreditation of the Animal Care and Use Committee of the Graduate School of Agricultural and Life Sciences, the University of Tokyo.

Surgical preparation and direct MCAO

Focal cerebral ischemia was induced by direct MCAO, involving the craniectomy technique [Fotheringham et al., 2000] with my modification. Established intraluminal thread methods [Clark et al., 1997; Kitagawa et al., 1998; Belayev et al., 1999; Kanemitsu et al., 2002; Wexler et al., 2002; Tsuchiya et al., 2003] occlude the ICA at the origin of the MCA (Fig. 1-1A), whereas the direct MCAO occludes a more distal portion of the MCA (Fig. 1-1B). In detail, anesthesia was induced by intraperitoneal administration of chloral hydrate (400 mg/kg body

weight in saline). Animals remained in anesthesia for 1.5-2 h before awaking. Temperature probes were inserted into the rectum and a heating pad was used to maintain rectal temperatures at 36.5 to 37.5 °C. The right MCA was exposed via the transtemporal approach. The skin between the lateral part of the orbit and the external auditory meatus was incised, and the upper part of the temporalis muscle was pushed aside after partial resection. A 1- to 2-mm burr hole was drilled using a leutor (Mini Gold; Nihon Seimitsu Kikai Kosaku Co,.Ltd., Hyogo, Japan) with a cemented carbide cutter (external diameter, 0.5 mm) (Nihon Seimitsu Kikai Kosaku Co,.Ltd.), through the frontal bone 1 mm rostral to the fusion of the zygoma and squamosal bone, and about 3.5 mm ventral to the dorsal surface of the brain (Fig. 1-1B). The MCA was exposed after the dura was opened and retracted. MCA was occluded by short coagulation with a general metallic heat applicator at a proximal location rather than in a branch (Fig. 1-1B), followed by transection of the vessel to ensure permanent disruption. The hole in the skull was sealed with dental cement (REPAIRSIN; GC Corp., Tokyo, Japan). After suturing, mice were returned to their cages in a controlled environment of 27-28 °C, where they were kept until sacrifice. Postsurgical survival was checked at 6, 12, and 24 h and 2, 4, and 8 day. Each experimental group consisted of four animals, except for the 24-h group. The 24-h group had fourteen animals for the comparison with CCAO, because I empirically observed the most developed lesions at this time point. Sham-operated animals (n=5) underwent the same procedure without occlusion and survived for 24 h. The operation was finished within 30 min.

Surgical preparation and CCAO

Unilateral CCAO was performed permanently or transiently to compare with direct MCAO. Anesthesia and maintenance of body temperature were performed as per the MCAO method. Through a small incision in the neck, the right common carotid artery was isolated from the vagal nerve and connective tissue by blunt dissection. Permanent CCAO (n=16) was performed by tightly knotting a 4-0 silk suture. Transient CCAO (n=8) was performed using an aneurysm clip applied unilaterally for 60 min, after which the clip was removed and blood flow through the vessel was confirmed. After occlusion, the neck incision was sutured. Postsurgical survival was checked at 24 h to compare with the peak lesions in the direct MCAO, then animals were sacrificed and the brain samples were obtained. Sham-operated mice (n=4) underwent the same procedure without CCAO and survived for 24 h.

Analysis of the Brain infarct lesion

After surgery, mice were sacrificed at each sampling points. Their brains were then removed and sectioned coronally at 2-mm intervals. For vital staining [Bederson et al., 1986], samples were incubated for 30 min in a 2% solution of 2,3,5-triphenyltetrazolium chloride (TTC; MP Biomedicals, Solon, OH, USA) at room temperature in the dark, fixed by immersion in 4% paraformaldehyde solution, and photographed. Image analysis was performed with the public domain Scion Image program (the U.S. National Institutes of Health; http://www.scioncorp.com/). Areas of infarction were plotted on tracings from projections of coronal sections, and infarct volume (InV), right hemisphere volume (RhV), and left hemisphere volume (LhV) were determined [Qi et al., 2004]. Infarct volume in each mouse was corrected

for hemispheric edema using the following formula: corrected infarct volume (CIV, %) = [LhV – (RhV – InV)]/LhV × 100.

Histological and immunohistological assessments

An additional two animals were perfusion fixed at 24 h, 4 and 8 day after direct MCAO and sham-operation, and postfixed with 4% paraformaldehyde in PBS (pH 7.4). Paraffin-embedded brains were sectioned at 10 μm. Hematoxylin and eosin (HE) staining was performed to identify morphologically normal and ischemic neurons as usual.

For immunohistological staining, the tissue specimens were autoclaved (10 min at 121℃) as a pretreatment. After blocking with Block Ace (Dainippon Sumitomo Pharma Co., Ltd., Osaka, Japan) for 60 min at room temperature, the specimens were labeled with polyclonal primary antibody to glial fibrillary acidic protein for astrocytes (GFAP: dilution 1:1000; Dako A/S, Glostrup, Denmark) and Iba-1 for microglias/macrophages (dilution 1:1000; Wako Pure Chemical Industries, Ltd., Osaka, Japan). Managed specimens were incubated at 4℃ overnight. The sections were then incubated with biotinylated goat anti-rabbit IgG (Dako A/S), which was followed by incubation with streptoavidin-biotin-horseradish peroxidase complex (sABC kit; Dako A/S). For visualization, 3,3-diaminobenzidine tetrahydrochloride (Sigma-Aldrich, Saint Louis, MO, USA) was used. Then, all sections were counterstained with hematoxylin.

In the analysis of BBB damage, I examined an extra-vessel infiltration of IgG in the infarct lesions. Anti-mouse IgG immunohistological staining was performed [Muramatsu et al., 1997]. Without a primary antibody, I used purified

biotinylated goat anti-mouse IgG antibody (Vector Labs, Burlingame, CA, USA) in place of a secondary antibody in the protocol.

Statistical analysis

All parameters are presented as mean ± SD. Student's t-test was used for CIV in the comparison of the ischemic group vs. the sham-operated group at 24 h after MCAO or CCAO. CIV values of each post-MCAO time group were analyzed by ANOVA followed by the post-hoc Tukey test. All statistical analyses used $P<0.05$ as the level of significance.

Results

Brain infarct lesions after direct MCAO

All mice treated with direct MCAO survived to each time point of 6, 12, and 24 h and 2, 4, and 8 day. I checked neurological scores in all animals after each surgery, but notable neurological deficits (circling, seizure and coma) were not observed. TTC staining was performed to measure infarct volumes in each group of the post-MCAO time point. Figure 1-2 shows infarct lesions at 24 h after direct MCAO. Brain samples were sectioned at bregma levels +0.62, -1.58, and -2.54 mm corresponding to the mouse brain atlas [Franklin and Paxinos, 1997]. The cortical area with infarct in the ipsilateral hemisphere was not stained with TTC. Sham-operated brain had no unstained areas, suggesting no visualized insult by craniectomy. To examine the potential hazards of the cauterization of the underlying brain tissue, I heated directly a part of cerebral cortex. At 24 h post-operation (the time of maximum lesions following direct MCAO), brain samples (n=3) were stained with TTC. Corresponding to the heated areas, the unstained areas had expanded to only 1 mm along the edges (data not shown). Therefore, the lesions following direct MCAO were demonstrated as being the result of ischemic insult, but not the heat insult.

To determine the temporal changes of lesions post-MCAO, the corrected infarct volume (CIV) was calculated for each time point (Fig. 1-3). At 6 h, an unstained area was observed (8.35 ± 1.93%), which gradually increased with time. CIV was maximal at 24 h (20.0 ± 5.0%) but had decreased at 2 day. However, substantial CIV was still noted until 8 day after MCAO (11.1 ± 2.6%). Statistical

significance was observed between groups of the post-MCAO time points in multiple comparisons.

Histopathological and immunohistological features

Histopathological examinations were performed to observe the ischemic features. The brains sampled 24 h after direct MCAO revealed the zones of cortical infarct lesion in the ipsilateral hemisphere (Fig. 1-4A). The infarct lesion was characterized by vacuolation and pancellular necrosis with dense eosinophilic areas, and shrunken neurons located along the edges of the infarct lesion (Fig. 1-4B). In the samples at 4 and 8 day, neuronal cells had decreased in the ischemic core zone and penumbra, whereas glial cells were frequently observed (data not shown).

In the immunohistological assessment, GFAP-positive astrocytes were diffusely located in unimpaired regions at 24 h (Fig. 1-5A). The samples obtained at 4 day showed GFAP-positive astrocytes which had increased in the areas surrounding infarct lesions, and showed hypertrophy and hyperplasia as features of "reactive astrocytosis" (Fig. 1-5B). The GFAP-positive processes of astrocytes were more developed in 8 day sample (Fig. 1-5C). On the other hand, Iba-1-positive cells, which are characterized as microglias and macrophages, infiltrated mildly into the ischemic core zone and penumbra at 24 h (Fig. 1-5D). At 4 day, Iba-1-positive cells had increased greatly in the penumbral region (Fig. 1-5E). Thereafter, the infarct lesion was completely inundated with considerable numbers of Iba-1-positive cells (Fig. 1-5F). Sham-operated mice showed neither features of activated glial cells nor increase of Iba-1 positive cells (data not shown).

Anti-IgG immunohistological staining was performed for IgG extra-vessel

inundation following direct MCAO. At 24 h, an anti-IgG immunoreaction was not emphatically observed (Fig. 1-5G). At 4 day, however, IgG exudation was found, moderately corresponding to the infarct lesion (Fig. 1-5H), and a strong anti-IgG immunoreaction was shown at 8 day (Fig. 1-5I).

Comparative analysis of direct MCAO and unilateral CCAO

Permanent and transient CCAO was performed unilaterally in order to compare with direct MCAO. I checked survival rates and the infarct lesions at 24 h after each operation, because the maximum areas of lesions following direct MCAO were observed at this time point. All mice (n=14) subjected to MCAO survived, while more than half of animals (10/16) and 2 of 8 animals died in the permanent and transient CCAO groups, respectively. The mortality rate was calculated by dividing the number of animals that died within 24 h after operation by the total number of animals in each group (Table 1-1).

The infarct occurrence rate was calculated by dividing the number of animals with ischemic insults by the number of surviving animals (Table 1-1). The MCAO reproducibly induced infarct lesion (100%), while permanent and transient CCAO groups showed lower rates, 50.0 and 66.7%, respectively.

Brain samples of the permanent CCAO model are shown at bregma levels -2.18 mm in Fig. 1-6. There was a variation of cerebral infarct-areas, namely including intense lesions extending to the cortex, hippocampus, and nucleus ventralis thalami (Fig. 1-6A), mild lesions limited to the cortex (Fig. 1-6B), and absence of lesions (Fig. 1-6C). Based on sections at 2-mm intervals, CIV was calculated using only samples with infarct lesion (Table 1-1). The CIVs of MCAO,

permanent and transient CCAO were 20.0 ± 5.0, 29.0 ± 28.8 and 33.2 ± 24.2%, respectively. Although both CCAO methods induced relatively large CIVs in comparison to MCAO, their SD was extremely high. Direct MCAO induced comparable infarct lesions, while large variation was observed in each CCAO group. CIV values of direct MCAO and transient CCAO were significantly higher than those of each sham-operated group (Table 1-1).

Discussion

The present study demonstrates the induction of infarct lesion by distal and proximal artery occlusion. Direct occlusion of the distal MCA was performed in C57BL/6 mice and was characterized by ischemic insults. In comparative analysis with unilateral CCAO, the distal MCAO consistently induced focal ischemic lesions in the ipsilateral hemisphere, whereas the unilateral CCAO models showed large variations of infarction. I convincingly demonstrated the efficiency of the direct method of the distal MCAO for the focal cerebral ischemic model.

The direct MCAO models induced infarct lesions, which extended to cortical areas. From the results of TTC staining, the CIV value reached a peak at 24 h and gradually decreased thereafter. Histological ischemic features were observed as vacuolation and shrunken neurons in the ischemic core and penumbral region at 24 h. In the immunohistological assessments, glial cell reactions were mainly observed at 4 and 8 day. It is considered that “reactive astrocytosis” might infiltrate for glial compensation and increase of Iba-1-positive cells (microglias/macrophages) might be for clearance of cellular debris gradually occurred. Accordingly these time points were on the transition from the acute to the chronic phase. Anti-IgG immunohistological staining revealed that BBB damage was continually induced for as long as 8 day following direct MCAO, although ischemic lesions were most developed with the edematous expansion at 24 h. A little is known about why BBB permeability changes maximally after ischemic edema has peaked. Nonselective BBB permeability would be related to passive leakage in necrotic vessels as previously indicated [Hatashita and Hoff, 1990]. Similar to my results, Lambertsen

et al. showed that infarct volume was maximal in SJL mice at 24 h in the direct-permanent MCAO model [Lambertsen et al., 2005]. On the other hand, the thread MCAO model has a different CIV peak. The thread-permanent MCAO induces peak CIV at 18 h in C57BL/6 mice, and at 24 h in rats [Wexler et al., 2002]. The difference in CIV peak time would be explained by differences of angioarchitectural anastomoses or speed of autolysis among rodent species [Yang et al., 1997; Kitagawa et al., 1999; Small and Buchan, 2000]. Additionally, my study and previous reports suggest that the CIV peak might change with the type (direct or indirect) of MCAO model.

The direct MCAO method induced ischemic lesions only in the cortical areas, corresponding to the distal MCA territory. On the other hand, it is likely that the intraluminal thread insertion induces more severe hemispheric ischemia, because of occlusion at the origin of MCA. Xi et al. [2004] reported that the direct ligation of MCA induced less expanded infarct volumes than those of intraluminal thread models. Recently, the intraluminal thread model was proposed to be an ICAO model rather than a simple MCAO model [Kanemitsu et al., 2002]. Intraluminal occlusion in rats produced damage in the cortex and caudate putamen within MCA territory and also in the hippocampus and thalamus as outside MCA territory [Kanemitsu et al., 2002]. In mice, the intraluminal thread occlusion leads to an occlusion duration-dependent [McColl et al., 2004] and filament thickness-dependent [Ozdemir et al., 1999] increase in extension of the ischemic lesion area outside MCA territory. Anomalies in the Circle of Willis are possibly a major cause for these ischemic lesions, and developed posterior communicating arteries (PcomAs) lead to a lack of uniformity in the insulted regions [Kitagawa et

al., 1998]. Collateral circulation in cerebrovascular anatomy would relate to variability of ischemic insults [Kelly et al., 2001; Maeda et al., 1998].

In the present study, I analyzed occlusion of the distal and proximal artery. The unilateral CCAO method, which I performed for proximal artery occlusion, is used for Mongolian gerbils [Matsumoto et al., 1988; Kitagawa et al., 1989; Hermann et al., 2001]. Mongolian gerbils lack PcomA which is necessary to complete the Circle of Willis, so this species has frequently been used to produce ischemic models [Small and Buchan, 2000]. Similarly, C57BL/6 mice are most susceptible to global ischemia corresponding to poor development of PcomA [Barone et al., 1993; Yang et al., 1997; Kitagawa et al., 1998; Kelly et al., 2001]. In my results, permanent and transient unilateral CCAO models had mortality rates of 62.5 and 25.0%, respectively. Unilateral CCAO induced severe ischemic insults in this strain. Meanwhile, mice surviving at 24 h post-CCAO showed severe to absent lesions. The permanent and transient CCAO models showed variability of CIV, 29.0 ± 20.8 and 33.2 ± 24.2%, respectively. I consider that the ischemic outcomes of unilateral CCAO cannot be constantly induced in the ipsilateral hemisphere. Kitagawa et al. reported that unilateral CCAO in C57BL/6 mice resulted in reduction of cortical microperfusion to 57.6 ± 7.9% of the baseline in the ipsilateral cerebral cortex, whereas bilateral CCAO reduced it to 4 to 7% [Kitagawa et al., 1998]. It is likely that the blood supply from contralateral CCA is partially redistributed to the ipsilateral cerebral circulation through the Circle of Willis, even in C57BL/6 mice. The possibilities of individual differences in PcomA or leptomeningeal anastomoses on the cortical surface remain [Barone et al., 1993; Kitagawa et al., 1998; Maeda et al., 1999; McColl et al., 2004]. It is necessary for more research into correlation of

blood flow and angioarchitectural anastomoses in unilateral CCAO mouse models in order to define the influences exerted by collateral circulation.

Direct occlusion of the distal MCA consistently induced ischemic lesions. All model animals (n=14) survived 24 h after MCAO and exhibited high reproducibility of infarct lesions (CIV=20.0 ± 5.0%). Ischemic insults of distal MCAO are limited to small areas compared to other types of proximal artery occlusion. In addition, occlusion of the distal location would have had a lesser influence on the collateral circulation, including PcomA [Barone et al., 1993; Kitagawa et al., 1998; Maeda et al., 1999] and the pterygopalatine artery [Tsuchiya et al., 2003; Tamaki et al., 2006]. This model could possibly be applied to the simple production of focal ischemia.

In the present study, I demonstrated the characters of the murine focal ischemic model by direct MCAO. With occlusion at the distal arterial portion, direct MCAO had high survivability and high reproducibility of infarct lesion within MCA territory. This method is more than adequate for the observation of ischemic insults, involving neuronal cell death, glial cell reactions and BBB damage. Moreover, direct MCAO can be performed without regard to variations in arterial augmentation or diameter that interfere with induction of consistent lesions in the intraluminal thread MCAO model. I consider that the direct MCAO method is appropriate for the analysis of cerebral infarction in senescent mice, which have enlarged arterial augmentation [Hartley et al., 2004]. In conclusion, direct MCAO is a very useful method for the induction of focal ischemic lesion in mice.

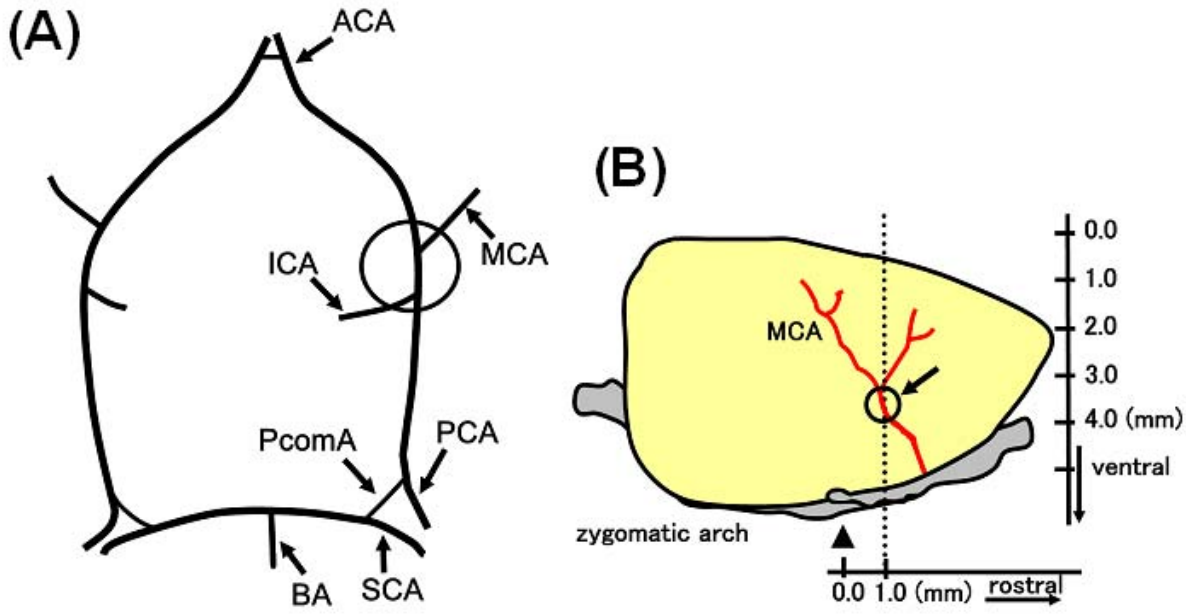

Fig. 1-1.

Schematic illustrations of the cerebral artery. (A) The Circle of Willis is formed by ACA, MCA and PCA, and supplies blood flow to the brain. The portion of the ICA to the origin of the MCA (surrounded by a circle) is the target of occlusion in intraluminal thread models. (B) Presentation of the direct MCA occlusion (MCAO) method. A 1- to 2-mm burr hole is drilled in the frontal bone; MCA is exposed and coagulated. The burr hole is represented by a circle (an arrow). This circle is located 1 mm rostral to the fusion (an arrowhead) of the zygoma and squamosal bone on the zygoma arch, and about 3.5 mm ventral to the dorsal surface of brain.

Abbreviations: anterior cerebral artery (ACA), middle cerebral artery (MCA), posterior cerebral artery (PCA), internal carotid artery (ICA), posterior communicating artery (PcomA), superior cerebellar artery (SCA) and basilar artery (BA).

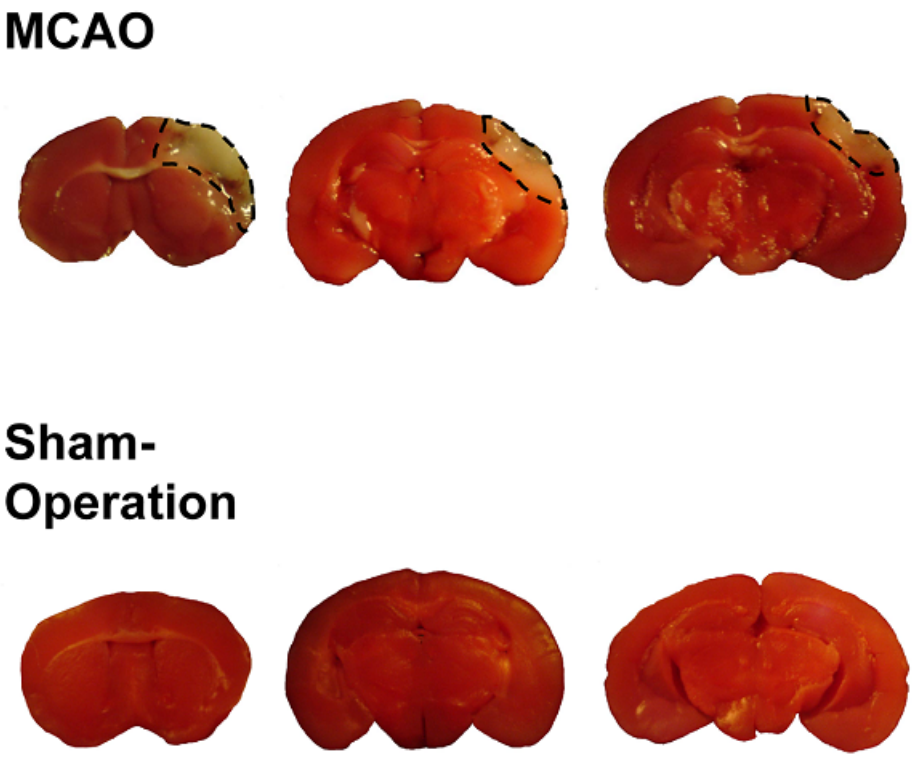

Fig. 1-2.

Triphenyltetrazolium chloride (TTC) staining of brain samples 24 h after direct MCAO (top) and sham operation (bottom) are shown. Brains were sectioned at the bregma level +0.62 (left), -1.58 (middle), and -2.54 mm (right).

Dotted lines surround unstained parts indicating infarct areas. Note the infarct lesions in the cortex of the right hemisphere.

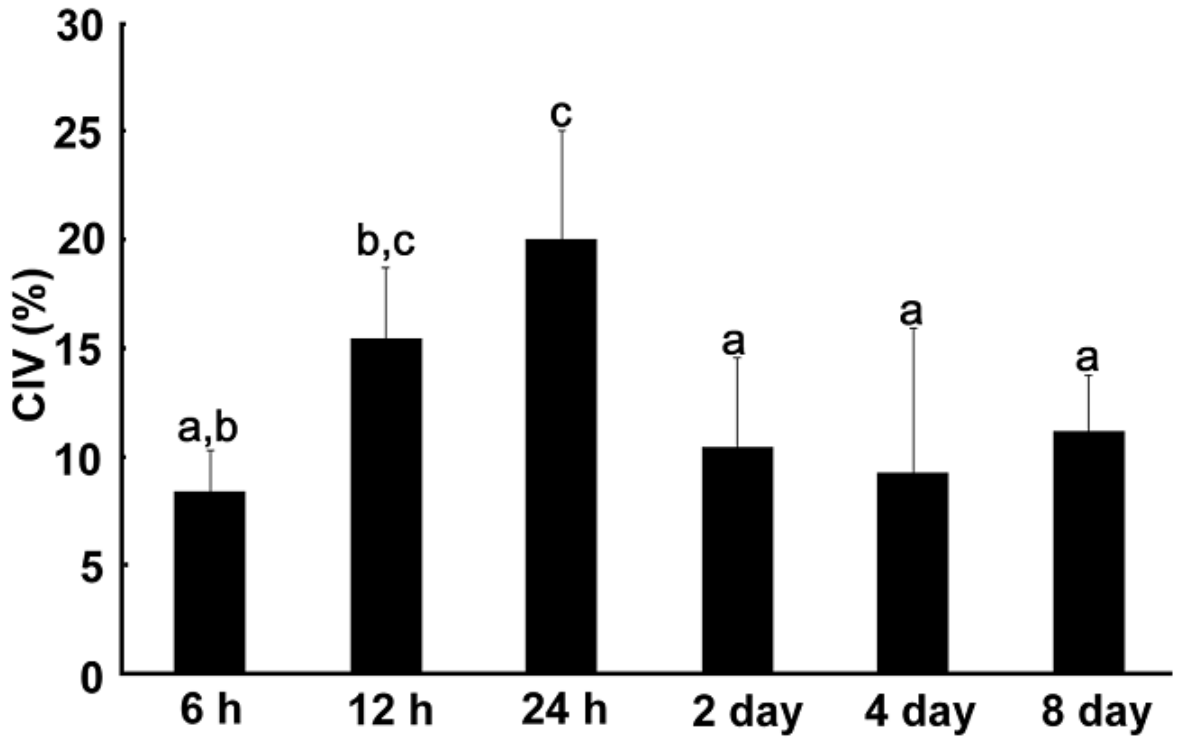

Fig. 1-3.

Changes in corrected infarct volume (CIV) and post-MCAO time.

Infarct lesions were visualized by TTC staining after direct MCAO. Each CIV value was calculated from sections at 2-mm intervals. CIV gradually increased in size and peaked at 24 h. Each experimental group had four animals, except for the 24-h group (n=14).

The post-hoc Tukey test was applied to the CIV value of each post-MCAO time group.

Values with different letters (a, b, and c) are significantly different (P<0.05) from each other.

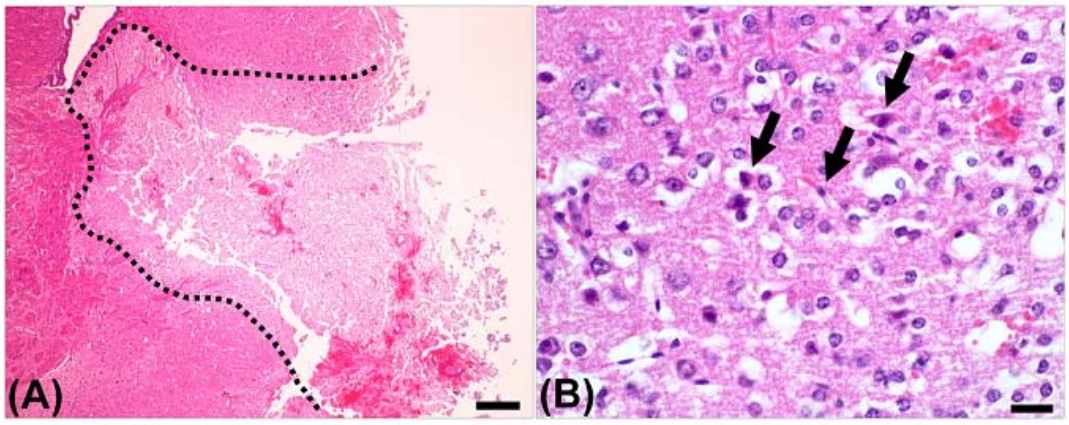

Fig. 1-4.

Histopathological features of the brain 24 h after direct MCAO.

(A and B) HE staining. Vacuolation and shrunken neurons were observed in cortical infarct lesions.

The dotted line in (A) surrounds an infarct lesion.

Arrows in (B) indicate shrunken neurons, which have eosinophilic cytoplasm.

Scale bars: (A) = 250 μm and (B) = 25 μm.

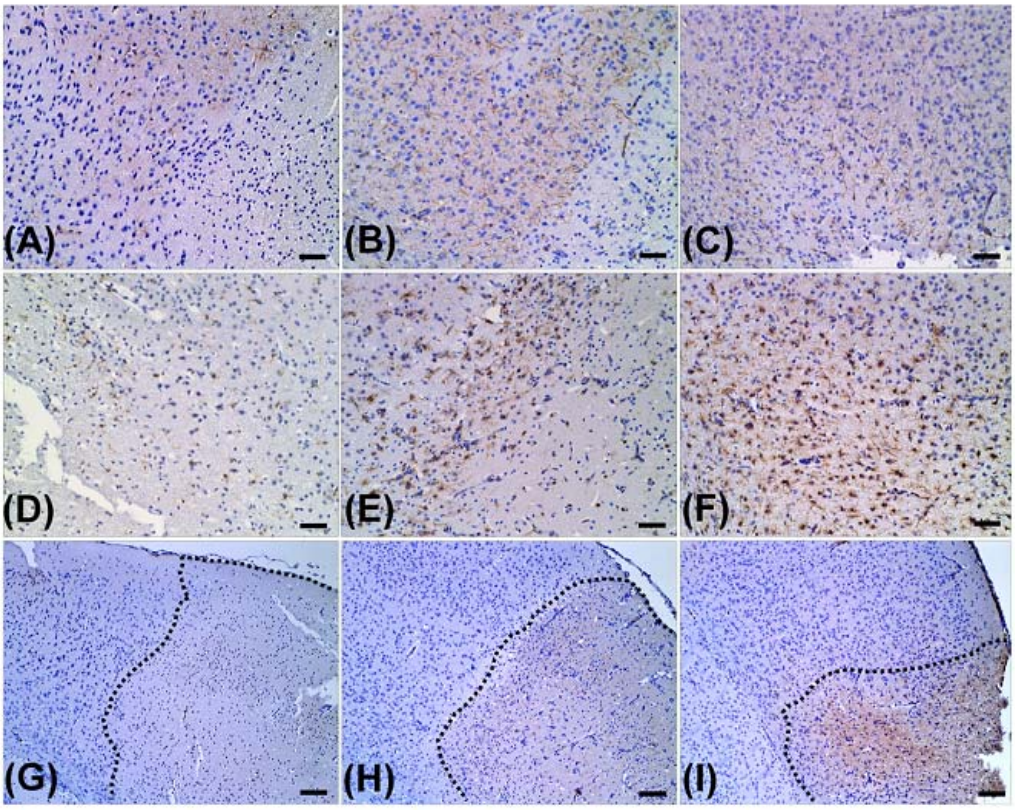

Fig. 1-5.

Immunohistological staining of cortical infarct lesions after direct MCAO. Glial cell reactions and IgG extravasation were examined by immunohistological staining with anti-GFAP (A-C), Iba-1 (D-F) and IgG (G-I) at 24 h (A, D and G), 4 (B, E and H) and 8 day (C, F and I).

Note that at 4 and 8 day hypertrophy and hyperplasia of GFAP-positive astrocytes were observed around infarct lesions, and that Iba-1-positive cells (microglias/macrophages) increase in the penumbral regions and ischemic core zones at 4 and 8 day, respectively.

An anti-IgG immunoreaction was observed corresponding to infarct lesions at 4 and 8 day. The dotted lines in (G-I) surround infarct lesions.

Scale bars: (A-F) = 50 μm and (G-I) = 100 μm.

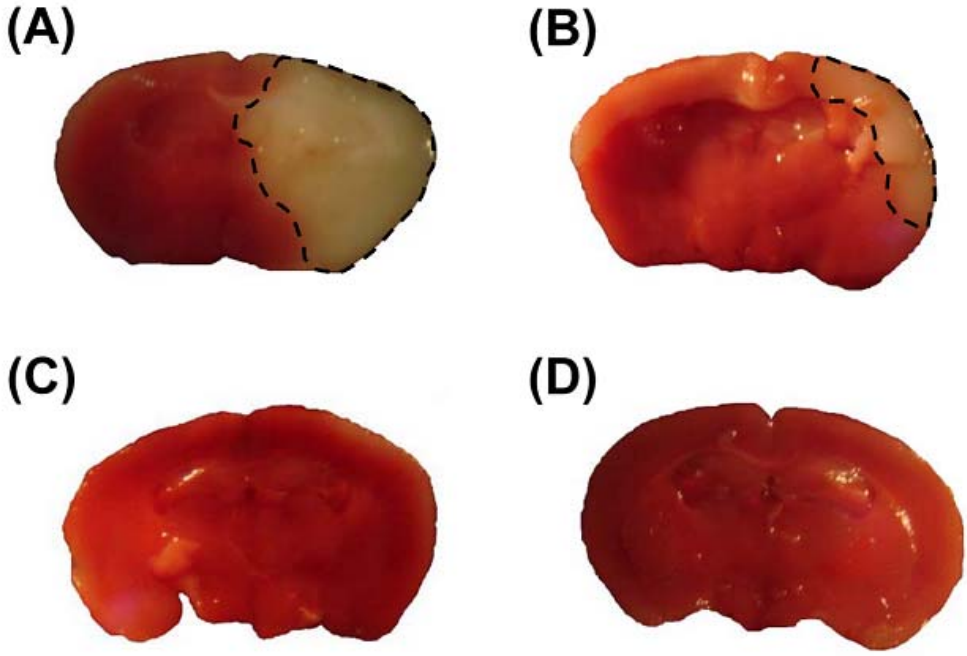

Fig. 1-6.

TTC staining of brain samples 24 h after permanent unilateral common carotid artery occlusion (CCAO). (A-C) Brain sections from the unilateral CCAO group and (D) sham-operation.

Infarct lesions exhibit marked variation in the unilateral CCAO group. Sections are shown at bregma level -2.18 mm.

Dotted lines surround unstained areas.

Table 1-1

Mortality rate, infarct occurrence rate and CIV at 24 hours after initiation of different types of unilateral artery occlusion

Occlusion type	Mortality rate (%)	Infarct occurrence rate (%)	CIV (%)
MCAO	0 (0/14)	100 (14/14)	20.0 ± 5.0**
Permanent CCAO	62.5 (10/16)	50.0 (3/6)	29.0 ± 28.8
Transient CCAO	25.0 (2/8)	66.7 (4/6)	33.2 ± 24.2#

Infarct occurrence rate was calculated by dividing the number of animals with infarct detected by TTC staining by the number of surviving animals. CIV was analyzed from only brain samples with infarct lesion. Values are the mean ± SD. **: $P<0.01$, #: $P<0.05$, compared to MCAO sham-operated group and CCAO sham-operated group, respectively (Student's t-test). CIV: corrected infarct volume. MCAO: middle cerebral artery occlusion. CCAO: common carotid artery occlusion.

Chapter 2

Analyses of the role of brain mast cell on expansion of infarct lesion at the acute stage of ischemia

Abstract

Despite the advances in the overall management of acute stroke, the propensity of ischemic brain tissue to develop swelling remains the major cause of death in patients with large infarctions. Hemispheric swelling is caused by brain edema following ischemia-induced cytotoxity and an increase in capillary permeability. Mast cells promote capillary permeability, through production of histamine, oxygen radicals and cytokines (e.g. TNF-α). Previously, it was shown that brain mast cells were activated following ischemic stroke, and influenced the early BBB failure and inflammation.

In the present study, I analyzed the roles of mast cell on expansion of infarct lesion at the acute ischemic stage. By using a murine permanent middle cerebral artery occlusion (MCAO) model, I applied the two patterned approaches: 1) early pharmacological modulation of mast cell (both inhibition and aggravation), 2) gene manipulated mast cell-deficient *W/W^v* mice and in their wild type. Both pharmacological mast cell stabilization state and absence of mast cell in *W/W^v* mice suppressed infarct volumes from 12 h to 2 day after permanent MCAO. And mast cell aggravation slightly increased expansion of infarct lesion against control groups. It is mentioned that brain mast cells participate in expansion of infarct lesion at the acute stage of brain ishcemia. In the initial lesion formation, the focal swelling would be strongly influenced whether mast cells are activated or stabilized, at least, before 12 h after brain ischemia.

Introduction

Despite the advances in the overall management of acute stroke, the propensity of ischemic brain tissue to develop swelling remains the major cause of death in patients with large infarctions [Hacke et al., 1996; Ayata and Ropper, 2002]. Brain swelling is harmful because of its effects on adjacent tissues and these effects are magnified by the fixed volume of the skull [Simard et al., 2007]. Swollen tissues exert a mechanical force on the surrounding shell of tissue, displacing it and increasing tissue pressure within it. As the intracranial pressure rises maximally at 24-72 h, cerebral perfusion pressure and cerebral blood flow are reduced to the levels that cannot support brain metabolism, and result in "brain death" [Rosenberg, 1999; Ayata and Ropper, 2002]. Accordingly, patients come under moribund threat, or to severe nervous disturbance at the chronic stage even if they escape death.

Hemispheric swelling is caused by brain edema following ischemia-induced cytotoxity and an increase in capillary permeability [Simard et al., 2007]. Movement of water contents and plasma proteins from a capillary into brain tissue is observed concomitant with the loss of autoregulation of the blood-brain barrier (BBB). Many factors including the hydraulic conductivity of capillaries, hydrostatic and osmotic pressure gradients, and tissue compliance and resistance, modify edema formation [Mayhan et al., 2001; Simard et al., 2007]. However, the pathophysiology of ischemic brain edema remains poorly understood.

It is known that some factors, such as histamine, oxygen radicals and cytokines (e.g. TNF-α), influence directly cerebral endothelial cells, and promote capillary permeability [Akassoglou et al., 1997; Rosenberg, 1999; Mayhan et al., 2001;

Ayata and Ropper, 2002]. Mast cells are the major source of these factors [Mayhan et al., 2001; Kakurai et al., 2006; Bischoff, 2007]. The ubiquity of mast cells in vertebrate brains has been well documented, at the perivascular and intraparenchymal sites of the cortex, hippocampus, thalamus, and hypothalamus [Grzanna and Shultz, 1982; Russell et al., 1990; Johnson and Krenger, 1992; Hendrix et al., 2006]. Similarly to other organs (lung, peritoneal, skin), brain mast cells regulate vascular permeability by selective release of mediators [Theoharides, 1990; Zhuang et al., 1996]. Because mast cells contain metachromatic granules which consist of substances such as vasoactive (histamine, bradykinin), anticoagulant (heparin), proteolytic (tryptase, chymase), and cytokines (TNF) [Gordon and Galli, 1991; Holgate, 2000], it is hypothesized that mast cells strongly influence the pathogenesis of brain ischemia.

In the previous study of transient global brain ischemia, the number of mast cells decreased in the thalamus 1 to 8 h after arterial occlusion, suggesting the result of ischemia-induced degranulation [Hu et al., 2004]. And cerebral mast cells promoted the BBB permeability and edema, and neutrophil infiltration 3 h after transient focal brain ischemia [Strbian et al., 2006]. These results are prominently involved at the early ischemic stage after brain ischemia, so that mast cells have a harmful influence to subsequent hemispheric swelling.

In the present study, I analyzed the roles of mast cell on expansion of infarct lesion at the acute ischemic stages, using a permanent middle cerebral artery occlusion (MCAO) model in mice. First, it was studied whether early pharmacological modulation of mast cell (both inhibition and aggravation) would influence brain ischemic damage following the process. In another set of

experiments, I performed permanent MCAO in gene manipulated mast cell-deficient WBB6F$_1$-*Kit*^{W}/*Kit*$^{W^v}$ (*W/Wv*) mice, and in their wild type (WT). *W/Wv* mice were often used in the studies of inflammatory mechanism, because they have little matured mast cells to carry a defective gene for c-kit (receptor for stem cell factor required for mast cell differentiation) [Kitamura and Hatanaka, 1978; Nocka et al., 1990]. By the two patterned approach, it is demonstrated that the possibility of deleterious change in brain ischemia is induced by brain mast cells.

Materials and Methods

Animals

C57BL/6 mice, and genetically mast cell-deficient *W/W^V* and the control WT mice (WBB6F$_1^{+/+}$) were purchased from Japan SLC, Inc (Shizuoka, Japan). I applied these murine strains (male, 10-13 weeks of age, 25-30 g) to permanent MCAO model. All animal care and experimentation were conducted in accordance with the guidelines of The University of Tokyo. All the experiments are conducted with an accreditation of the Animal Care and Use Committee of the Graduate School of Agricultural and Life Sciences, the University of Tokyo.

Pharmacologic Protocols

I examined the effects of pharmacological mast cell modulation on brain infarct lesions in C57BL/6 mice, by either cromoglycate or compound 48/80 (C48/80). The cromoglycate (cromolyn sodium; Sigma-Aldrich Co., St. Louis, MO, USA) is a clinically used inhibitor of mast cell degranulation, and topically administered at concentration of 75 μg/ml in saline. Cromoglycate solution (4 μl) was injected into the cerebral ventricle because of minimal crossing to the BBB, and vehicle (250 μl) was intraperitoneally injected. The C 48/80 (MP Biomedicals, Solon, OH, USA) is a standard mast cell degranulating secretagogue, and prepared at a concentration of 0.5 mg/ml saline. C48/80 solution (250 μl) was injected intraperitoneally, and vehicle (4 μl) was injected into the cerebral ventricle. In control group, mice were injected vehicle (only saline) both intracerebroventricularly and intraperitoneally. Five min after each injection, all animals were received permanent MCAO or

sham-operation.

Surgical preparation and permanent MCAO

Focal brain ischemia was induced in pharmacologic injected C57BL/6 mice, and both *W/W^v* and WT mice. Permanent occlusion of the middle cerebral artery (MCA) was performed as mentioned in Chapter 1. Postsurgical survival was checked at 12 and 24 h, and 2 and 4 day. Each experimental group consisted of five animals. Furthermore, sham-operated animals (n=3 per each group) underwent surgical procedures without arterial occlusion, and survived for 24 h.

Analysis of the brain infarct lesion

After surgery, mice were sacrificed. Their brains were then removed and sectioned coronally at 2-mm intervals. Samples were incubated for 30 min in a 2% solution of 2,3,5-triphenyltetrazolium chloride (TTC; Sigma-Aldrich Co.) at room temperature in the dark, fixed by immersion in 4% paraformaldehyde solution, and photographed. Image analysis was performed with the public domain Scion Image program (the U.S. National Institutes of Health; http://www.scioncorp.com/). Areas of infarction were plotted on tracings from projections of coronal sections, and infarct volume in each mouse was calculated from the total amount of infarct areas in each section.

TNF-α measurement

I detected serum TNF-α to determine the effects of pharmacological mast cell modulation. C57BL/6 mice were divided into 4 injection groups (n=3), including

vehicle-, C 48/80-, cromoglycate- and cromoglycate with additional C 48/80-injected groups. Injection protocols were as above mentioned, except for cromoglycate with additional C 48/80-injection group. In the protocol of cromoglycate with additional C 48/80-injection, mice were injected with C 48/80 intraperitoneally following intracerebroventricular injection of cromoglycate. Thirty min after each injection, blood samples were obtained from the heart as sacrificed. Samples were centrifuged and the serum was stored at -80 °C. TNF-α measurement was performed with standard enzyme-linked immunosorbent assay (ELISA) kit according to the manufacturer's instructions: Amersham TNF-α Mouse, Biotrak ELISA system (sensitivity 10 pg/ml) (GE Health care UK Ltd., Little Chalfont, Buckinghamshire, England).

Histopathological and immunohistological assessments

After analysis for the infarct volume of permanent MCAO-induced brain samples in WT and *W/W^v* mice, the samples were destained with TTC, and used for histopathological and immunohistological assessments (n=2). Paraffin-embedded brains were sectioned at 10 μm. Hematoxylin and eosin (HE) staining was performed to identify morphologically normal and ischemic neurons as usual.

To observe glial cells changes, immunohistological staining was performed in ischemic brain samples. The sections were autoclaved (10 min at 121℃) as a pretreatment. After blocking with Block Ace (Dainippon Sumitomo Pharma Co., Ltd., Osaka, Japan) for 60 min at room temperature, the specimens were labeled with polyclonal primary antibody to glial fibrillary acidic protein for astrocytes (GFAP: dilution 1:1000; Dako A/S, Glostrup, Denmark) and Iba-1 for

microglias/macrophages (dilution 1:1000; Wako Pure Chemical Industries, Ltd., Osaka, Japan). Managed specimens were incubated at 4℃ overnight. The sections were then incubated with biotinylated goat anti-rabbit IgG (Dako A/S), which was followed by incubation with streptoavidin-biotin-horseradish peroxidase complex (sABC kit; Dako A/S). For visualization, 3,3’-diaminobenzidine tetrahydrochloride (Sigma-Aldrich, Saint Louis, MO, USA) was used. Then, all sections were counterstained with hematoxylin.

Statistical analysis

All parameters are presented as mean ± SD. Dunnett's test was used for all the comparison, except for infarct volume analysis in *W/W^V* and WT mice. Values of Infarct volume in *W/W^V* and WT mice were analyzed by Student's t-test. All statistical analyses used $P<0.05$ as the level of significance.

Results

Brain infarct lesions in pharmacologically mast cell-modulated mice

All mice treated with permanent MCAO survived to each time point of 12 and 24 h, and 2 and 4 day. As the characteristic of this MCAO at the distal portion, I observed no neurological deficits (circling, seizure and coma) in all animals. TTC staining was performed to measure infarct volumes of each pharmacologic injection group. Figure 2-1 shows infarct lesions of vehicle, C 48/80 or cromoglycate injected mice at 24 h after MCAO. Represented sections were indicated frontal cortex to caudal at 2 mm-intervals. The infarct area in cortex of the ipsilateral hemisphere was not stained with TTC. In C 48/80-injected group, infarct lesions were swelling and more expanded than those of vehicle-injected group (Fig. 2-1A, B). On the other hand, cromoglycate-injected group had limited the expansion of infarct lesions, and no lesion in caudal cortex (Fig. 2-1A, C). Sham-operated brains had no unstained areas, except for the traces of needle injection (data not shown).

To compare the temporal changes of lesion in each group, the infarct volume was calculated (Fig. 2-2). At 12 h unstained areas were observed, and were maximal at 24 h. Thereafter, the values of infarct volume slightly decreased. C 48/80-injected group had comparably the higher values of infarct volume than those of vehicle-injected group, although statistical significance was not detected totally except for 4 day samples. In contrast, cromoglycate-injected group had the smaller values than those of vehicle-injected group, especially at 24 h and the statistically significant decrease was observed.

Determination of pharmacological mast cell-modulation

In order to determine the effects of pharmacological injection for mast cell-modulation, serum TNF-α measurement was performed. Increase of serum TNF-α was recognized as the indicator of activated mast cells [Gordon and Galli, 1991]. Among all the injection groups, C 48/80 injection induced alone serum TNF-α product (Fig. 2-3). Similarly to vehicle-injected group, cromoglycate injection resulted in no detection of serum TNF-α, even followed C 48/80 injection. These results suggested that C 48/80 or cromoglycate pharmacologically modulated mast cells to activation or stabilization, respectively.

Brain infarct lesions in mast cell deficient mice

Mast cell deficient *W/W^V* and WT mice were treated with permanent MCAO, and survived to each time point of 12 and 24 h, and 2 and 4 day. Infarct lesions, which were not stained with TTC, were shown at 24 h after MCAO (Fig. 2-4). Represented sections were indicated frontal cortex to caudal at 2 mm-intervals. Brain samples in WT mice had infarct areas expanding caudal cortex (Fig. 2-4A). In contrast, *W/W^V* mice were shown less expanded lesions (Fig. 2-4B). Each sham-operated brain sample had no staining areas (data not shown).

I compared the infarct volume of WT and *W/W^V* mice at each time point (Fig. 2-5). Similarly to the results of pharmacological mast cell-modulation experiments, infarct lesions were maximal at 24 h, and then slightly decreased from 2 day. WT mice showed drastically increased infarct volume from 12 to 24 h, whereas values in *W/W^V* mice increased at little amplitude. And infarct volumes of *W/W^V* mice were significantly decreased when compared with those of WT mice, at 12- and 24h- and

2 day-post-MCAO.

Histopathological and immunohistological features

Histopathological examinations were performed to observe the ischemic features. The brains in WT and *W/W^V* mice 24 h after MCAO revealed no difference in ischemic core zone (Fig. 2-6). Infarct lesion was characterized by vacuolation and pancellular necrosis with dense eosinophilic areas, and shrunken neurons located along the edges of the infarct lesion.

In the immunohistological assessments, changing of GFAP-positive astrocytes were also observed as similar features in both WT and *W/W^V* mice (Fig. 2-7). GFAP-positive astrocytes were located in unimpaired regions at 12 h (Fig. 2-7A, E), and slightly increased at 24 h (Fig. 2-7B, F). At 2 day, GFAP-positive astrocytes largely increased in number at the areas surrounding infarct lesions (Fig. 2-7C, G), and showed hypertrophy and hyperplasia as features of "reactive astrocytosis" at 4 day (Fig. 2-7D, H).

The features of Iba-1-positive cells, which were characterized as microglias and macrophages, differed between WT and *W/W^V* mice (Fig. 2-8). At 12 and 24 h, in WT mice Iba-1-positive cells infiltrated moderately into the ischemic core zone and penumbra, whereas infiltration of these cells in *W/W^V* mice was mildly observed (Fig. 2-8A, B, E, F). Thereafter, Iba-1-positive cells had increased greatly in the penumbral region in both WT and *W/W^V* mice at 2 day (Fig. 2-8C, G). And at 4 day, many numbers of Iba-1-positive cells intensely infiltrated from the penumbral region into ischemic core zone (Fig. 2-8D, H).

Discussion

In the present study, I analyzed the roles of mast cell on expansion of ischemic lesion. Mast cells are stationary cellular mediators of immediate hypersensitivity and show local phlogistic reactions to mechanical, toxic, and allergic stimuli [Grimbaldeston et al., 2006; Bischoff, 2007]. I show that brain mast cells participated in expansion of infarct lesion. Both pharmacological mast cell stabilization state and absence of mast cell in the gene-manipulated *W/W^v* mice strongly suppressed expansion of infarct lesion from 12 h to 2 day after brain ischemia. In my permanent MCAO model, expanded lesions were peaked at 24 h with induction of the focal swelling, and gradually calmed. In human patients, cytotoxic and vasogenic edema is maximal at 24-72 h after acute ischemic stroke [Rosenberg, 1999]. Therefore, the present MCAO model had acute ischemic process similarly to the human disorder. It is considered that effects of brain mast cells exert at the acute stage of ischemia.

Strbian et al. [2006] reported that pharmacological degranulation of mast cell promoted ischemic BBB permeability, brain swelling and neurtrophil infiltration, in rat MCAO model with 60 min of ischemia followed by 3 h of reperfusion. It was mentioned that brain mast cells had influences post-ischemic BBB failure and inflammation at the early stage. My experimental results of expansion of infarct lesions at 12 h to 2 day were akin to their report. It was discussed that formation of initial infarct lesion, which was promoted or inhibited corresponding to mast cell modulations, impacted on subsequent lesion development. In C 48/80 injection group, however, ischemic injuries were slightly

more expanded than those of vehicle injection group. These results would have been reflected by degrees of mast cell activation. In the previous studies, prior C 48/80 injection acted strongly on early ischemic changes [Strbian et al., 2006], whereas general ischemic strokes in animals seemed to induce gradually mast cell activation. In adult and neonatal rat brains, mast cell degranulation was shown 1-8 h after transient global ischemia and 24 h after permanent MCAO, respectively [Hu et al., 2004; Biran et al., 2008]. My permanent MCAO model showed that infarct volumes of vehicle group were already close to those of C 48/80 group at 12-24 h, suggesting likely plateau of mast cell activation. There are some differences among rodent species, aging and ischemic models, but my study and previous reports support the hypothesis that brain mast cells are gradually activated and participate in ischemic development, according to the cellular localization closely to ischemic core.

The mechanism of mast cell activation in ischemia is unclear. However, as well as plasma extravasation in BBB damage in stroke and subarachnoid hemorrhage, complement components C3a and C5a are yielded which are the most potent stimulators of mast cell [Lindsberg et al., 1996]. And adenosine, that dramatically increased under ischemia as consequence of energy metabolism failure, activates mast cells via A_3 adenosine receptor [Ramkumar et al., 1993; Latini and Pedata, 2001; Rossi et al., 2007].

As one theory in permanent ischemic models, on maximal edema at 24 to 48 h, the increase in water was likely caused by cytotoxic edema rather than the promoted permeability [Rosenberg, 1999]. I consider that brain mast cells also relate with disruption of the BBB integrity. The BBB integrity is largely determined by basal lamina, the three main constituents of which are the matrix proteins

laminin, fibronectin, and collagen type IV. The integrin-labled basal lamina loses its integrity very early after ischemic onset [Tagaya et al., 2001]. Mast cells release the matrix metalloproteinase (MMP)-2 and MMP-9, which degrade collagen type IV [Fang et al., 1999]. And secreting granules of the brain mast cells contain chymase and a potent protease which cleaves fibronectin and also activates procollagenases [Saarinen et al., 1994; Tetlow et al., 1998], even in the presence of the tissue inhibitor of metalloproteinase-1 [Frank et al., 2001]. Thus, mast cell-derived enzymes may participate in post-ischemic basal lamina degradation, and disruption of the BBB integrity.

In both pharmacological mast cell stabilization state and absence of mast cell in *W/W^v* mice, from 12 h to 2 day after MCAO, the expansion of infarct lesion was suppressed, whereas slightly approached to control groups at 2-4 day. Following the maximal expansion, brain mast cells might have little effects on subsequent process. On the other hand, mast cells have potentially roles on neuroprotection. Neurotrophic and/or tropic cues (e.g. nerve growth factor) could be produced directly by mast cells [Leon et al., 1994]. And histamine suppresses the ATP depletion during ischemia by preventing energy consumption [Adachi et al., 2005]. Possibly, brain mast cells may have a good function at the chronic stage of brain ischemia. It is necessary for more detailed examinations in the long term.

In the histopathological examination, 24 h after permanent MCAO in *W/W^v* mice had no different features from WT mice in ischemic core zone and penumbral area; vacuolation, pancellular necrosis and shrunken neurons. It is suggested that brain mast cells exert no effects of morphological changes in necrotic or apoptotic neurons. Similarly, in both *W/W^v* and WT mice, an increase in number of astrocytes

was equally shown in the areas surrounding infarct lesions at 12 h-2 day, and subsequent “reactive astrocytosis” at 4 day. On the other hand, infiltration of Iba-1 positive cells (macrophages/microglias) in *W/W^v* mice was milder than those in WT mice at 12-24 h, although subsequent infiltration was equal to WT. From these results, I considered one possibility that mast cells also participated in initial activation of macrophages/microglias at the early ischemic stage via proinflammatory cytokines (e.g. TNF-α, IL-1) release. Eventually, activation and migration of macrophages/microglias would be recruited with attraction by neuronal death [Thomas, 1992], or the interactions with astrocytes [Tanuma, et al., 2006].

In conclusion, brain mast cells have roles on expansion of infarct lesion at the acute stage. I consider that in initial formation of the infarct lesions, the focal swelling is strongly influenced whether mast cells are activated or stabilized, at least, before 12 h after brain ischemia. As a therapeutic treatment, stabilization of brain mast cells could be a new target at the early ischemic onset.

Fig. 2-1.

Infarct lesions in pharmacologically mast cell-modulated mice. Triphenyltetrazolium chloride (TTC) staining of brain samples from vehicle (A), C 48/80 (B) and cromoglycate (C) injected mice at 24 h after MCAO. Brains were sectioned frontal cortex to caudal at 2 mm-intervals. Dotted lines surround unstained parts indicating infarct areas. Each cortical infarct lesion is shown to compare with vehicle injected mice. C48/80 injected mice had swelling and expanded infarct lesions, whereas cromoglycate injection induced less expansion and no lesion in caudal cortex.

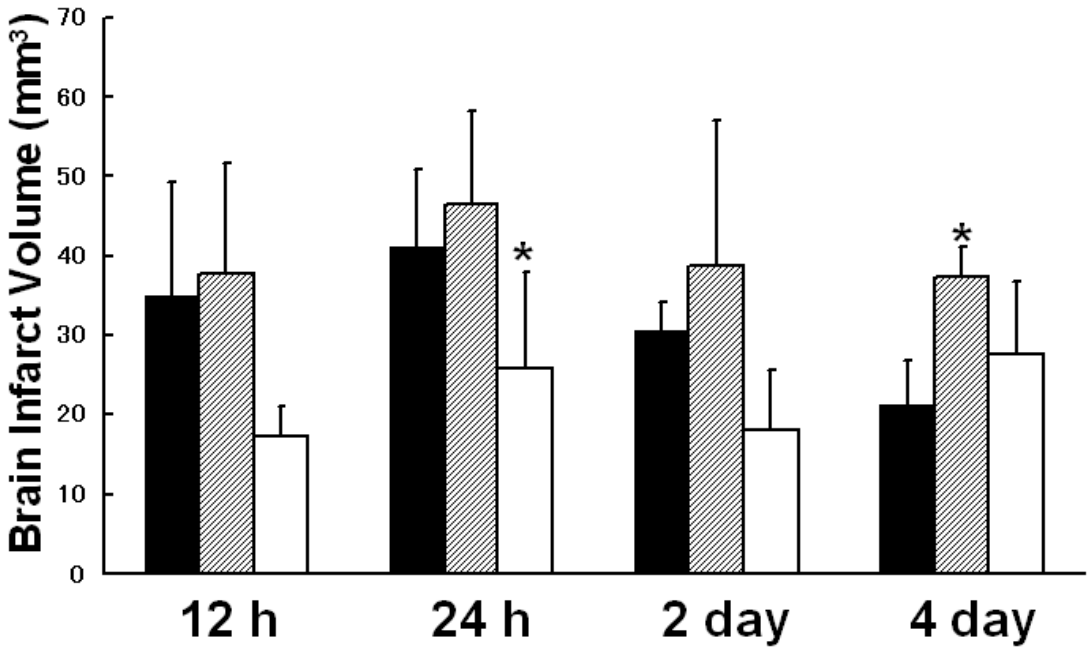

Fig. 2-2.

Changes of infarct volume and post-MCAO time in pharmacologically mast cell-modulated mice. Vehicle (control) (black bars), C 48/80 (oblique line bars) and cromoglycate (white bars) are shown.

Infarct volumes were peaked at 24 h, and had decreased from 2 day. C 48/80 injection had comparably the higher values, whereas cromoglycate injection induced small infarct volumes.

Dunnett's test was applied to the values of injection groups each post-MCAO time. Values are significantly different (P<0.05) from vehicle injected group.

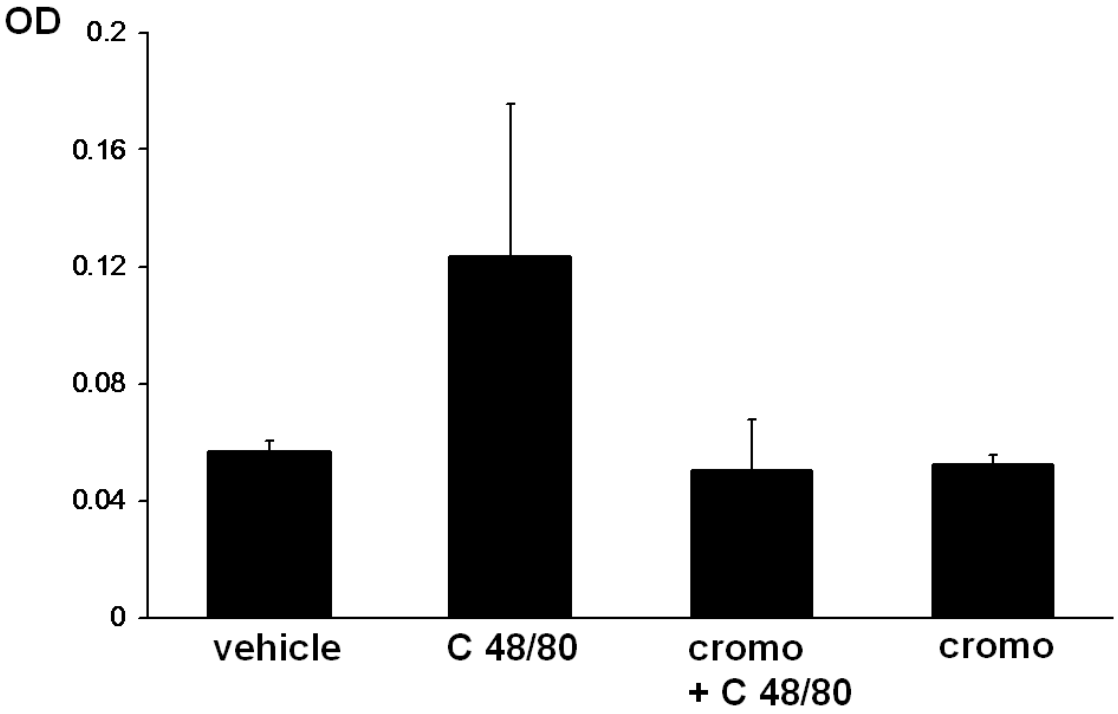

Fig. 2-3.

Serum TNF-α measurement after pharmacological mast cell-modulation. C 48/80 injection induced increase of serum TNF-α, suggesting mast cell activation. In other injection groups, expression of serum TNF-α was not detected.

Fig. 2-4.

Infarct lesions in mast cell deficient *W/W^V* mice. TTC staining of brain samples from WT (A) and *W/W^V* (B) mice at 24 h after MCAO. Brains were sectioned frontal cortex to caudal at 2 mm-intervals.

Dotted lines surround unstained parts indicating infarct areas.

W/W^V mice had less expanded lesions than WT mice.

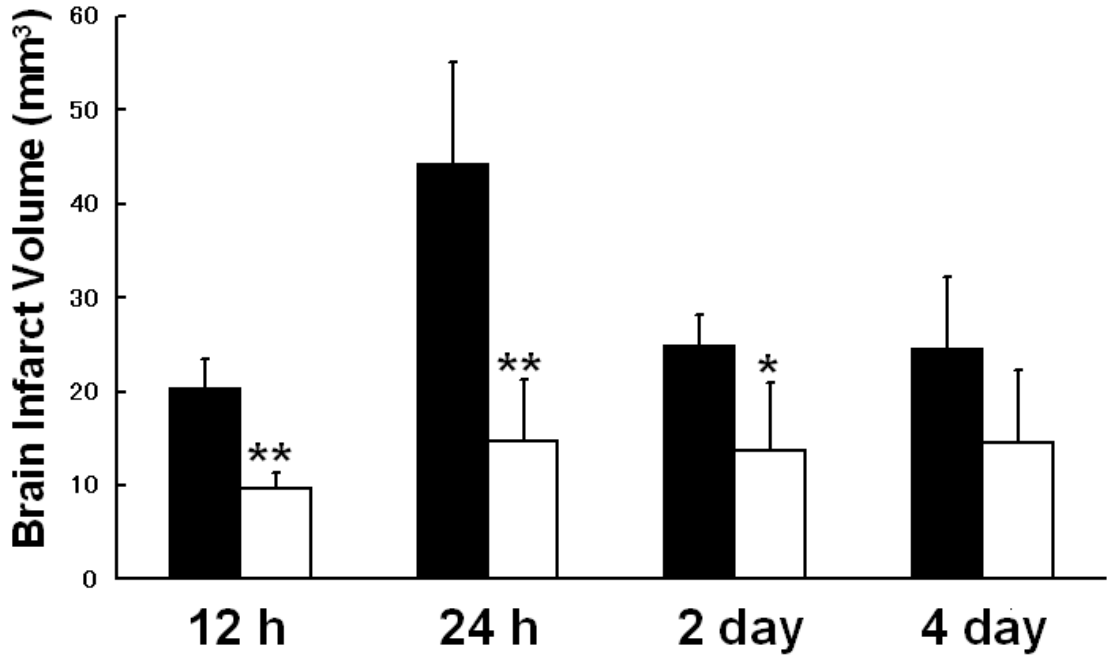

Fig. 2-5.

Changes of infarct volume and post-MCAO time in mast cell deficient *W/W^V* mice. Values of infarct volume in WT (control) (black bars) and *W/W^V* (white bars) mice are shown.

Infarct volumes of *W/W^V* mice were totally decreased compared with those of WT mice.

Student's t-test was applied to the values of injection groups each post-MCAO time. Values are significantly different ($P<0.05$) from WT mice.

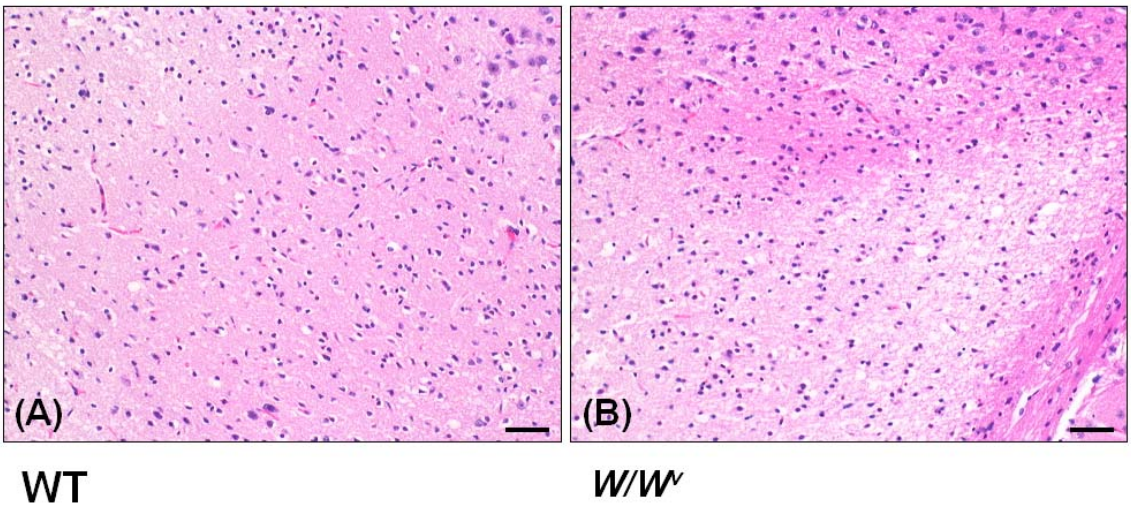

Fig. 2-6

Histopathological features of the brain in *W/W^V* mice 24 h after MCAO. HE staining in WT (A) and *W/W^V* (B) mice.

In cortical infarct lesions, vacuolation and shrunken neurons were observed in both WT and *W/W^V* mice.

Scale bars: 50 μm.

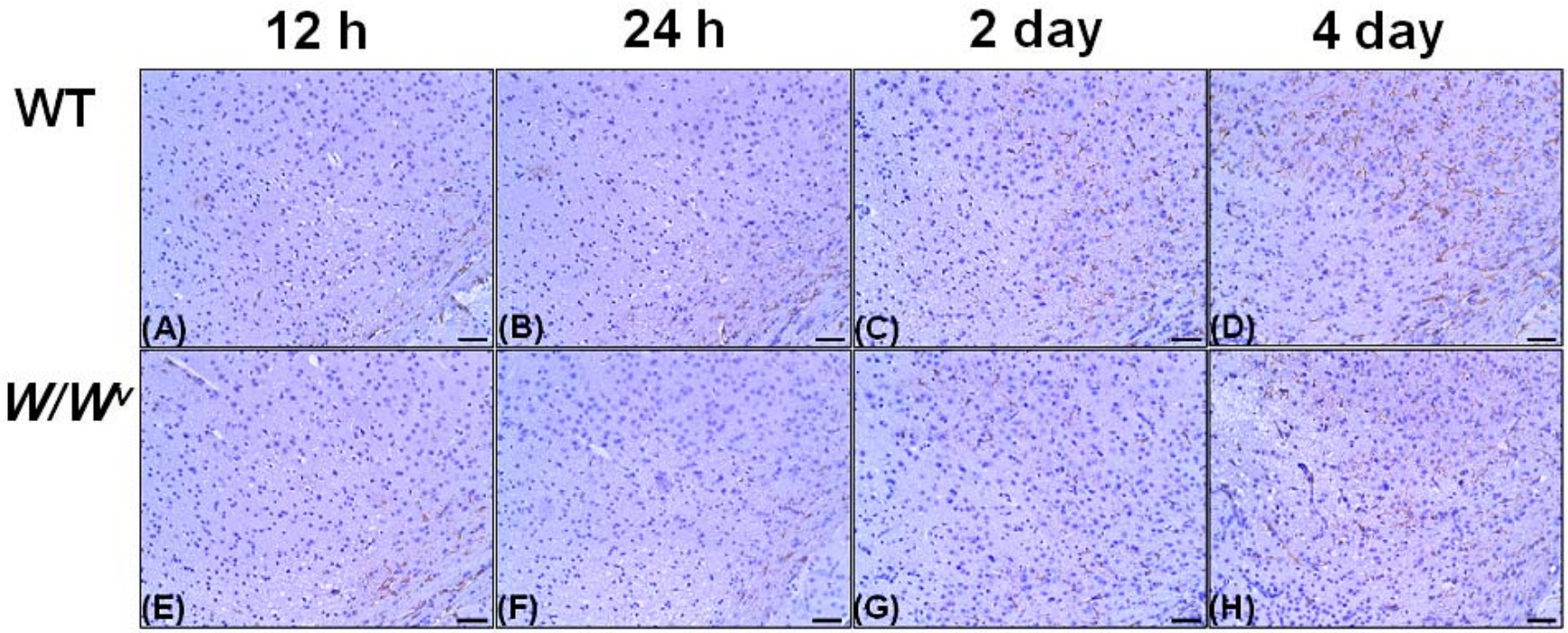
12 h
24 h
2 day
4 day
WT
W/Wv
(A)
(B)
(C)
(D)
(E)
(F)
(G)
(H)

Fig. 2-7.

Immunohistological staining with anti-GFAP in WT (A-D) and *W/W^V* (E-H) murine brains after MCAO. Astrocytic reaction was examined at 12 h (A and E) and 24 h (B and F), and 2 day (C and G) and 4 day (D and H). Note that at 4 day hypertrophy and hyperplasia of GFAP-positive astrocytes were observed around infarct lesions in both WT and *W/W^V* mice.

Scale bars: 50 μm.

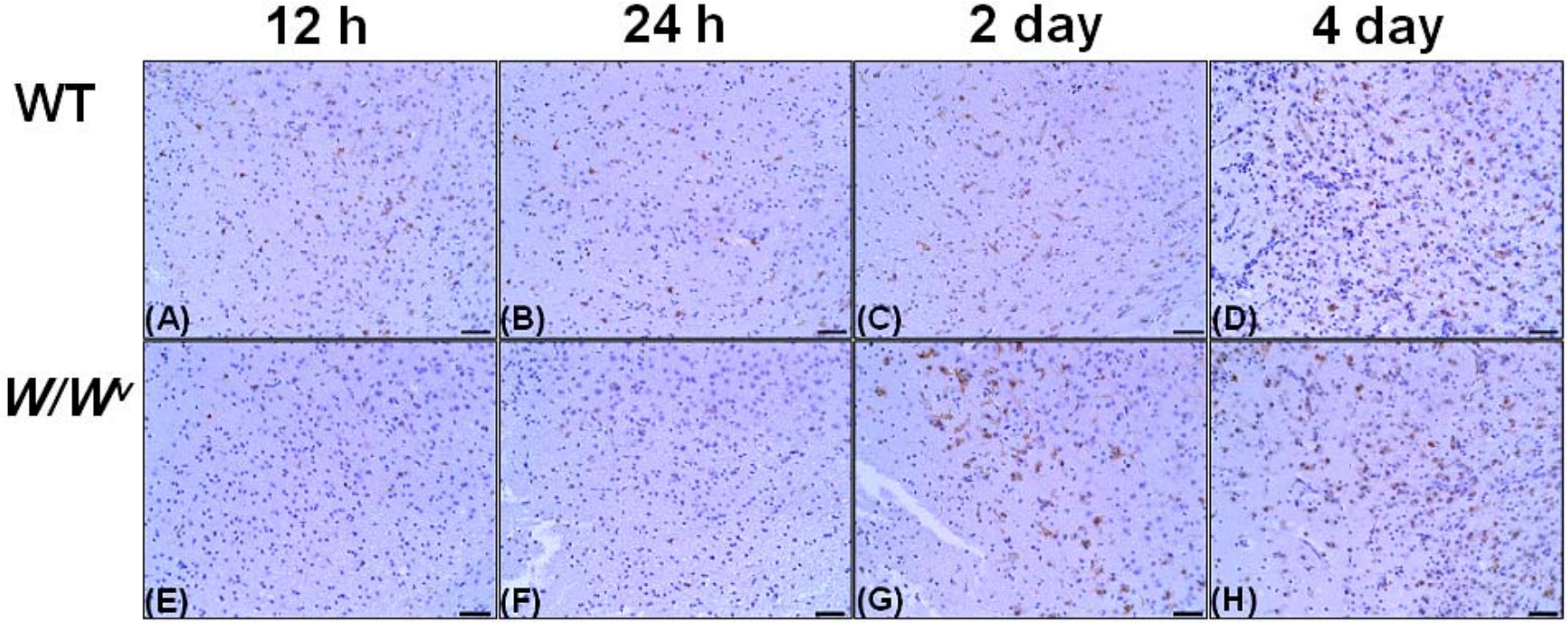
12 h
24 h
2 day
4 day
WT
W/Wv
(A)
(B)
(C)
(D)
(E)
(F)
(G)
(H)

Fig. 2-8.

Immunohistological staining with anti-Iba-1 in WT (A-D) and *W/W^V* (E-H) murine brains after MCAO. Increase of Iba-1-positive cells (microglias/macrophages) was examined at 12 h (A and E) and 24 h (B and F), and 2 day (C and G) and 4 day (D and H).

Iba-1-positive cells gradually increased in the penumbral region and ischemic core zone. Note that at 12 and 24 h in *W/W^V* mice infiltration of Iba-1-positive cells was milder than that in WT mice.

Scale bars: 50 μm.

Chapter 3

Analyses of matrix metalloproteinase expression after global ischemia in mast cell-deficient (*W/Wv*) mouse

Abstract

Matrix metalloproteinases (MMPs) are expressed as zymogens that cleave protein components of the extracellular matrix and a number of cell surface targets. Excessive or inappropriate expression of MMPs can contribute to pathologic processes of brain ischemia in close association with the breakdown of the blood-brain barrier (BBB) and the neuroinflammatory response. In relation of MMP system, I focused attention on mast cell functions. Brain mast cells have been shown to activate after ischemia, and contribute to ischemic processes promoting BBB permeability and inflammation.

To define mast cell functions in the implication of MMP, I analyzed global ischemic model in mast cell-deficient WBB6F$_1$-*Kit*^{W}/*Kit*$^{W\text{-}v}$ (*W/Wv*) mice. At 24 h after global ischemia in *W/W*^{v} mice, both neurological deficits and ischemic areas were limited, and BBB damage was remarkably reduced when compared with those of wild type (WT) mice. By zymography analysis, active MMP-9 was increased in brains obtained from WT mice, detecting immunohistological expression of cortical neurons, glial cells and infiltrated neutrophils. While *W/W*^{v} mice were shown the reduction of MMP-9 expression and the results were reflecting decrease of MMP-9 positive neurons.

It was suggested that brain mast cells increase active MMP-9 expression in surviving neurons, probably through inflammatory stimuli. This role is discussed that mast cells indirectly promote BBB damage via MMP system at the acute stage of ischemia.

Introduction

Matrix metalloproteinases (MMPs) belong to a rapidly growing family of enzymes which have been identified to date more than 20 members. They are Zn^{2+}-dependent endopeptidases, including gelatinases, collagenases, stromelysins and membrane-type MMPs [Chandler et al., 1996; Murphy et al., 1999]. The MMPs are expressed as zymogens that are activated upon proteolytic cleavage of a propeptide. The MMPs cleave proteins of extracellular matrix, but also process a number of cell surface proteins such as receptors, pro-inflammatory cytokines and other soluble proteins. The proteolytic activity of MMPs is controlled by the tissue inhibitors of metalloproteinase (TIMPs), a family of secreted multifunctional proteins that comprises four members (TIMP-1 to TIMP-4), with 30-40% sequence similarity each other [Greene et al., 1996; Cunningham et al., 2005]. All TIMPs inhibit the active forms of most MMPs by forming noncovalent 1:1 complexes with them.

Excessive or inappropriate expression of MMPs can induce pathologic processes, and it is well known that alterations in the expression and activity of MMPs are linked to the development of several brain diseases. Increased levels of MMPs have been found in degenerative disorders such as multiple sclerosis, Alzheimer's, and Parkinson's diseases [Anthony et al., 1997; Asahina et al., 2001; Lorenzl et al., 2002]. Recently, neurologists have gained interest in the potential implication of MMPs in the pathophysiology of brain ischemia. The MMP-2 (gelatinase A) and MMP-9 (gelatinase B) are up-regulated in rodent brains after global and focal ischemia [Romanic et al., 1998; Rosenberg et al., 2001; Rivera et al.,

2002; Magnoni et al., 2004], in close association with the breakdown of the blood-brain barrier (BBB) and the neuroinflammatory response [Rosenberg et al., 1998; Cunningham et al., 2005]. Furthermore, MMP-9 gene knockout mice have been shown to reduce the infarct volume and BBB disruption after transient focal ischemia [Asahi et al., 2001]. These evidences suggest that MMPs, in particular gelatinases MMP-2 and -9, might contribute to ischemic damage but little is known about their mechanisms.

In relation to pathological/inflammatory processes of MMPs, I focused my attention on mast cell functions. Mast cells are being recognized as sentinels of innate immunity and modulators of adaptive immunity, through the release of biologically highly active cytokines, chemokines, lipid mediators, proteases and biogenic amines [Heib et al., 2008]. Brain mast cells have been shown to activate after ischemia, and contribute to ischemic processes as shown in Chapter 2 and previous reports [Hu et al., 2004; Jin et al., 2006; Strbian et al., 2006; Biran et al., 2008]. The present series of experiments were performed to define mast cell functions in increased MMP expression. Additionally, I investigated the pathophysiological characters of the MMPs in global ischemic model with gene manipulated mast cell-deficient WBB6F$_1$-*Kit*^{W}/*Kit*$^{W^v}$ (*W/Wv*) mice.

Materials and Methods

Animals

Genetically mast cell-deficient *W/W^{V}* and the control WT mice (WBB6F$_1^{+/+}$) were purchased from Japan SLC, Inc (Shizuoka, Japan). I applied these murine strains (male, 10-13 weeks of age, 25-30 g) to global ischemic model. All animal care and experimentation were conducted in accordance with the guidelines of The University of Tokyo. All the experiments are conducted with an accreditation of the Animal Care and Use Committee of the Graduate School of Agricultural and Life Sciences, the University of Tokyo.

Surgical preparation and common carotid artery occlusion

To induce global ischemia, bilateral common carotid artery occlusion (bCCAO) was performed. Anesthesia and maintenance of body temperature were performed as per the MCAO method (Chapter 1, 2). Through a small incision in the neck, bilateral common carotid artery was isolated from the vagal nerve and connective tissues by blunt dissection. The bCCAO was transiently performed using an aneurysm clip applied for 15 min, after which the clip was removed and blood flow through the vessel was confirmed. After reperfusion, the neck incision was sutured. Postsurgical survival was checked at 24 h, and brain samples were obtained. Sham-operated mice underwent the same procedure without bCCAO and survived for 24 h.

Measurement of neurological deficits

Mice were tested and divided into 4 grades for neurological deficits as follows: normal as no detectable neurological deficit; mild as failure to extend forepaw fully and/or a decline of spontaneous walking; moderate as circling and/or loss of spontaneous walking; severe as coma or dead. Assessments were made at 24 h after the bCCAO.

Measurement of ischemic areas

Mice (n = 5 per each group) were killed 24 h after ischemic onset. Five coronal sections per brain (2-mm-thick) were prepared and stained with 2,3,5-triphenyltetrazolium chloride (TTC; Sigma-Aldrich Co.), followed fixation of 4% paraformaldehyde solution. Image analysis was performed with Scion Image program (the U.S. National Institutes of Health). Ischemic areas were plotted on tracings from projections of coronal sections, and the rate of ischemic area was calculated as follows: The rate of ischemic area (%) = total ischemic area/total hemispheric area × 100.

Assessment of blood-brain barrier damage

To visualize BBB leakage, animals (n = 3 per each group) were received a 2% solution of Evans blue albumin (fluorescent dye, 20 mg/mL dissolved in 1% albumin) into the tail vein (0.12 mL/40 g B.W.), 30 min before cardiac perfusion. Mice were perfusion-fixed at 24 h after the bCCAO, and postfixed with 4% paraformaldehyde. Brains were removed, and stored at -20℃.

Frozen 20-μm serial coronal sections were cut from the macroscopically

determined epicenters of the Evans blue-stained brain lesions and air-died for up to 2 h. All the sections were then examined for distribution of characteristic red fluorescence of Evans blue in the brain parenchyma by an epifluorescent microscope (BX-FLA; Olympus Corporation, Tokyo, Japan) with a fluorescence filter (U-MWIG; Olympus Corporation). For evaluation of BBB damage, images of three certain cortical regions in the ischemic area were measured, as well as reference images from the area of control mice. I quantified Evans blue-albumin fluorescent pixels with Scion Image program (the U.S. National Institutes of Health). The level of autofluorescence was based on that obtained from the area of control mice. For each animal, I calculated the difference between the fluorescence signal in three selected region images and the level of autofluorescence. Finally, the corrected signals from all three images were averaged.

Preparation of tissue extracts

At 24 h after the onset of ischemic insult, mice (n = 3 per each group) were decapitated. Sham-operated control mice similarly killed at 24 h. Brains were removed quickly and divided into the cortex, striatum, hippocampus and thalamus.

Each tissue was frozen immediately in liquid nitrogen and stored at -80℃. Brain samples were homogenized in 10 × volume lysis buffer (CelLytic MT Mammalian Tissue Lysis/Extraction Reagent; Sigma-Aldrich), including protease inhibitor (Protease Inhibitor Cocktail; Sigma-Aldrich) on ice using a Teflon glass homogenizer. After centrifugation (13,000 rpm) for 10 min at 4℃, the supernatant fluid was collected. Total protein concentration of each sample was determined using the Lowry method.

Gelatin zymography

To confirm the activation of MMP-9, gelatin zymography was performed. Briefly, each tissue extracts were mixed with one-part of 2 × Tris-glycine SDS sample buffer [12.5 mM Tris-0.5 M HCl, pH 6.8, 20% glycerol, 4% SDS (w/v), and 0.005% bromophenol blue (w/v)], and the mixtures were left at room temperature for 10 min. The samples (total protein; 50 μg/well) were applied on a 10% polyacrylamide gel containing 0.1% gelatin, and the gel was electrophoresed with Tris-glycine SDS electrode buffer according to standard running conditions. After running, the gel was first incubated with zymogram renaturing buffer [2.5% Triton X-100 (v/v)] with gentle agitation for 30 min at room temperature. Then the gel was incubated in fresh zymogram renaturing buffer [0.02% Brij-35 (v/v)] for 72 h at 37℃ for maximum sensitivity. Coomassie blue (0.5%; w/v) in fixative [methanol/acetic acid/water (50:10:40)] was used for visualizing the areas of protease activity, followed by destaining [methanol/acetic acid/water (50:10:40)]. Recombinant murine MMP-9 and MMP-2 (Sigma-Aldrich) were used as positive controls. To quantify the relative levels of MMP-9 expression, the gels were scanned, and the mean band intensity (per mm^2) was quantified with analysis software (Quantity One Ver. 4.5; Bio-Rad Laboratories, Hercules, CA, USA).

Immunohistological assessments

Mice were perfusion-fixed at 24 h after bCCAO (n = 3) or sham-operation (n = 2), and postfixed with 4% paraformaldehyde. Paraffin-embedded brains were sectioned at 10 μm. The tissue specimens were autoclaved (10 min at 121℃) for MMP-9 or treated with 8M guanidine in 0.1M Tris-HCl buffer, pH7.6 (at room

temperature for 24 h) for TIMP-1. After blocking with Block Ace (Dainippon Sumitomo Pharma Co., Ltd., Osaka, Japan) for 60 min at room temperature, the specimens were mounted each primary antibody. I labeled the specimens with antibodies as follows: polyclonal rabbit primary antibody to MMP-9 (dilution 1:250; Sigma-Aldrich) and TIMP-1 (dilution 1:100; Sigma-Aldrich), and monoclonal mouse primary antibody to MMP-2 (dilution 1:100; Daiichi Fine Chemical Co., Ltd., Toyama, Japan). Managed specimens were incubated at 4℃ overnight. The sections were then incubated with biotinylated goat anti-rabbit IgG (Dako A/S) or goat anti-mouse IgG antibody (Vector Labs, Burlingame, CA, USA), which was followed by incubation with streptoavidin-biotin-horseradish peroxidase complex (sABC kit; Dako A/S). For visualization, 3,3 ' -diaminobenzidine tetrahydrochloride (Sigma-Aldrich) was used. Then, all sections were counterstained with hematoxylin.

Statistical analysis

All parameters are presented as mean ± SD. Student's t-test was used for all the comparisons, except for MMP-9 activity. To compare MMP-9 activity, band intensity values of gelatin zymography were analyzed by Dunnett's test. All statistical analyses used $P<0.05$ as the level of significance.

Results

Neurological deficits

Ischemia-treated or sham-operated mice were divided into 4 grades of neurological deficits; normal, mild, moderate and severe (Table 3-1). In the groups of global ischemia at 24 h, The WT mice had the highest rate in the severe grade, and secondary in the moderate. On the other hand, mast cell-deficient *W/W^V* mice were most frequent in the moderate grade. It was indicated that neurological deficits of *W/W^V* mice had been totally more alleviated than those of WT mice. Sham-operated groups in both WT and *W/W^V* mice had no neurological deficits. I applied ischemic-treated mice, which showed moderate or severe neurological deficits, to the following experimentations.

Measurement of ischemic areas

At 24 h after bCCAO, brain samples were stained with TTC solution to analyze ischemic areas. Figure 3-1A shows ischemic areas of WT and *W/W^V* mice. Represented sections indicated the frontal and parietal cortex portions. The ischemic areas in the bilateral hemispheres were not stained with TTC. In WT mice, ischemic lesions were observed in the frontal and parietal cortex and the striatum, and parts of the hippocampus and thalamus. On the other hand, *W/W^V* mice had limited the expansion of ischemic lesions, the frontal and parietal cortex and the striatum. Total ischemic areas of five sections from each mouse were shown (Fig. 3-1B). Ischemic lesions in WT mice tended to expand more than those in *W/W^V* mice, although statistic significance was not detected.

Blood-brain barrier damage

Mice were injected Evans-blue albumin intravenously to analyze the BBB damage 24 h after bCCAO. In WT mice the surface of brain sample was partially stained with Evans-blue, suggesting extravasation of Evans-blue albumin (Fig. 3-2A). While *W/W^V* mouse brain was not shown visualizing staining. On a fluorescent microscope, red fluorescent Evans-blue dye was detected prominently on vessel walls, and perivascular areas (Fig. 3-2B, C). In WT mice, fluorescence was strongly observed in perivascular areas and neuron-like-cell rich areas, while that of *W/W^V* mice had weakly appeared. When compared with WT mice, the number of fluorescence pixels indicating magnitude of extravasation was significantly reduced in *W/W^V* mice (Fig. 3-3).

Gelatin zymography

The bands of gelatinolytic activity were present in the cortex of ischemic and sham-operated mice (Fig. 3-4A). The 105 kDa and 72 kDa bands were suggestive of the active forms of murine MMP-9 and MMP-2, respectively. After global ischemia, changes in MMP-9 gelatinolytic activity were conspicuous with respect to sham-operated mice. Levels of MMP-9 increased significantly or slightly in WT (265%) and *W/W^V* mice (146%) to each sham-operated mouse group, respectively (Fig. 3-4B). When compared with ischemic WT mice, ischemic *W/W^V* mice were significantly reduced at the nearly half level. On the other hand, the bands of active MMP-2 were faint or little detectable in all groups (Fig. 3-4A). Similar changes after global ischemia was observed in the striatum, hippocampus and thalamus (data not shown).

Immunohistological assessments

In sham-operated groups in both WT and *W/W^V* mice, MMP-9 immunolabling was not detected (data not shown). After global ischemia, in WT mice cortical neurons in the peri-ischemic areas were positive for MMP-9 (Fig. 3-5A, B). *W/W^V* mice, however, had few immunoreacted neurons (Fig. 3-5C, D). Otherwise, in both WT and *W/W^V* mice MMP-9 positive cells were morphologically identified as glial cells and infiltrated neutrophils (data not shown). MMP-2 immunoreaction was detected very occasionally in a part of vascular walls in both ischemic and sham-operated mice (data not shown).

I also performed immunohistological staining anti-TIMP-1, which was recognized as the inhibitor of MMP-9. In both ischemic WT and *W/W^V* mice, TIMP-1 immunoreaction was diffusely detected in neurons and blood vessel walls (Fig. 3-6A, B). These features were slightly more frequent than those of sham-operated mice (data not shown).

Discussion

In the present study, I analyzed MMP expression level in global ischemic model using mast cell-deficient *W/W^v* mice. Concomitant with the reduced MMP-9 expression in *W/W^v* mice, both neurological deficits and ischemic areas were limited, and BBB damage was remarkably reduced when compared with those of WT mice. These results indicated that mast cells also participated in pathophysiology of transient global ischemia, as well as transient and permanent focal ischemia [Strbian et al., 2006; Chapter 2 in this paper]. At the early ischemic stage, brain mast cells are activated and influence BBB permeability and inflammation [Hu et al., 2004; Strbian et al., 2006; Jin et al., 2007; Brian et al., 2008]. In Chapter 2, I observed that mast cells promoted significantly the focal expansion of the brain lesions after middle cerebral artery occlusion (MCAO). In the present global ischemic model, however, ischemic lesion areas of *W/W^v* mice were very slightly milder than those of WT mice. This global ischemic model induced more severe ischemic insults than those of MCAO. Thus, I considered that the effects of mast cell would be obscurely shown on the expansion of ischemic lesions in this model.

In *W/W^v* mice, BBB permeability was intensely reduced because of showing low extravasation of Evans-blue albumin. Evans-blue albumin is often used as a macromolecule tracer which indicates the BBB advanced permeability and damages [Nakagawa et al., 1990; Warnick et al., 1995; Strbian et al., 2008]. I considered that mast cells would contribute BBB permeability through release of many vasoactive agents, such as TNF-α, histamine, serotonin, prostaglandins, leukotriens, platelet-activating factor, and nitric oxide [Zhuang et al., 1996; Steiner et al., 2003],

as well as potent contributions of secretory granules containing MMPs and chymase which disrupted the BBB integrity [Saarinen et al., 1994; Tetlow et al., 1998; Fang et al., 1999].

Active MMP expression analyses were performed to detect whether MMPs expression was related with tempered insults in *W/W^v* mice. At 24 h after global ischemia, active MMP-9 was increased in brains obtained from WT mice. Immunohistologically, I observed that cortical neurons, glial cells and infiltrated neutrophils were the source of MMP-9. By zymography analysis, *W/W^v* mice were shown the reduction of MMP-9 expression and the results were reflecting decrease of MMP-9 positive neurons. It was suggested that in *W/W^v* mice inflammatory stimuli might be weak against neuronal cells by loss of mast cell functions. MMPs expression is stimulated by proinflammatory cytokines, especially TNF-α, as well as expression of other inflammatory cytokines and adhesion molecules [Chandler et al., 1997; Rosenberg et al., 1995]. After brain ischemia, TNF-α production was observed in neurons, microglias, astrocytes and ependymal cells [Gong et al., 1998; Lambertsen et al., 2005]. Similarly, brain mast cells would be also the candidate of TNF-α production cell [Cocchiara et al., 1998; 1999]. From my experimentation results, it was discussed that brain mast cells might have a role of indirect promotion of BBB damage by inducing MMP production, as well as direct operations on BBB by secretary mediators.

At 24 h after global ischemia, in WT mice MMP-9 expression was observed in neurons, glial cells and neutropils, while MMP-2 positivity was rarely detected in a small number of blood vessel walls. Similar features were previously reported. MMP-9 was expressed by neurons and neutrophils at 24-48 h, and thereafter by

microglias, astrocytes and macrophages [Rosenberg et al., 2001; Rivera et al., 2002; Magnoni et al., 2004]. MMP-2 expression was lately promoted in astrocytes, macrophages and vessel walls at 3-21 day [Romanic et al., 1998; Rosenberg et al., 2001; Rivera et al., 2002; Magnoni et al., 2004]. These differences would be involved in cell viability and tissue remodeling in the ischemic brains. To examine the relation of mast cells and MMP-2 expression, it is necessary for long-term study.

TIMP-1 was expressed by neurons and blood vessel walls in both WT and *W/W^{v}* mice. It was suggested that TIMP-1 expression would be potentially independent from mast cells related stimuli. In rat global ischemic model, TIMP-1 was shown in neurons and astrocytes, suggesting neuroprotective reaction against ischemic insults [Rivera et al., 2002]. Differences in cellular expression might be according to the degrees of ischemic insults, occlusion time-dependence and/or angioarchitectural-dependence.

In conclusion, brain mast cells increase active MMP-9 expression in surviving neurons, probably through inflammatory stimuli. This role is suggested that mast cells indirectly promote BBB damage via MMP system. Thus at the acute stage of brain ischemia, the insult would be intensely processed with participation of multi functions in mast cell.

Table 3-1

Neurological deficits (%)

	Normal	Mild	Moderate	Severe
WT-Isch	18 (5/28)	11 (3/28)	21 (6/28)	50 (14/28)
WT-Sham	100 (5/5)	0	0	0
W/W^{v}-Isch	17 (4/24)	8 (2/24)	42 (10/24)	33 (8/24)
W/W^{v}-Sham	100 (5/5)	0	0	0

Mice were divided into 4 grades of neurological deficits. Abbreviations: Isch, Ischemia-treated; Sham, Sham-operation-treated.

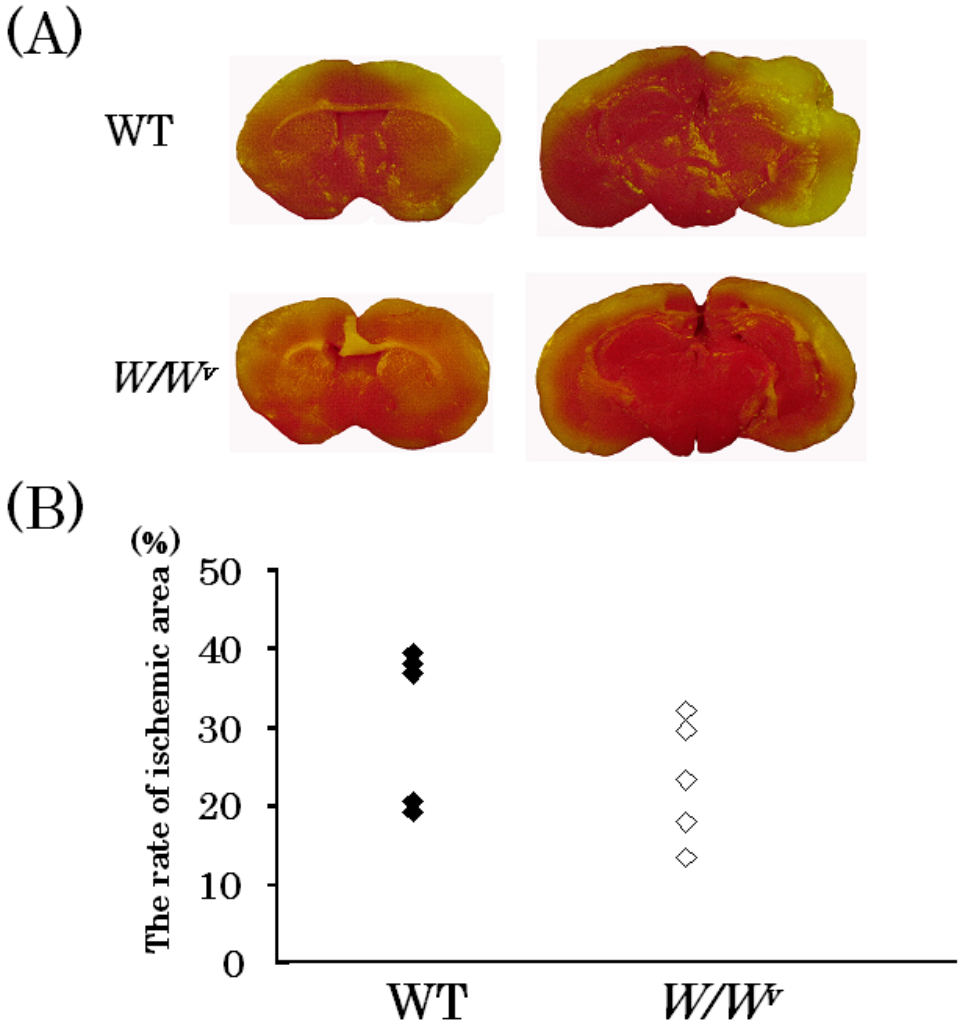

Fig. 3-1.

Ischemic lesions in mast cell deficient *W/W^V* mice. (A) TTC staining of brain samples from WT (top) and *W/W^V* (bottom) mice at 24 h after bCCAO. Represented sections are shown the frontal (left) and parietal (right) cortex portions. The ischemic areas in the bilateral hemispheres were not stained with TTC. Note that *W/W^V* mice had less expanded lesions than WT mice.

(B) Changes of total ischemic areas. The rates of ischemic area in WT (control) (black diamonds) and *W/W^V* (white diamonds) mice are shown. Ischemic lesions of *W/W^V* mice tended to decrease compared with those of WT mice.

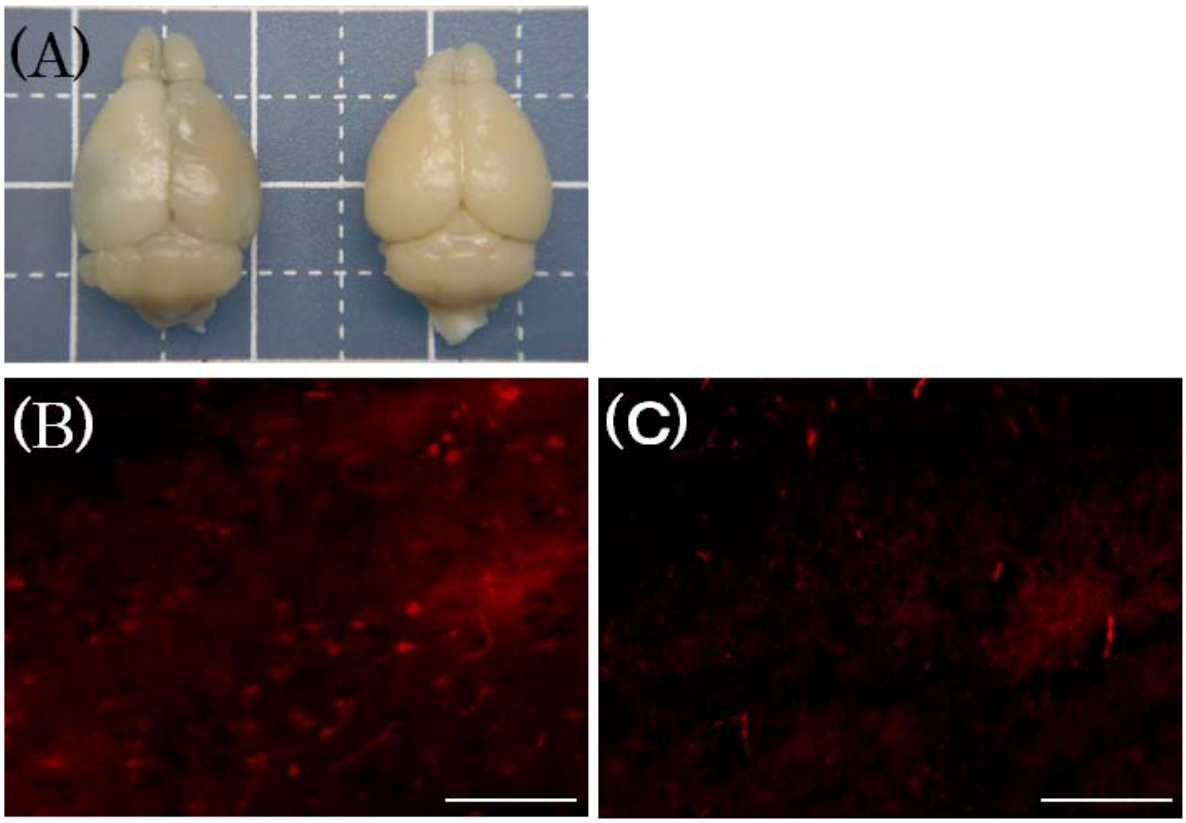

Fig. 3-2.

Blood-Brain barrier (BBB) damage in *W/W^V* mice.

(A) Brain samples from WT (left) and *W/W^V* (right) mouse, which were injected Evans-blue albumin intravenously.

Note that in WT mice the surface of brain was partially stained with Evans-blue.

(B, C) Microscopy showing Evans-blue fluorescent signal in tissue sections of ischemic lesions, reflecting the floridity of extravasation of particles of albumin size. (B) WT and (C) *W/W^V* mouse. Extravasation is punctuated, focusing on small vessels or their endothelia. In WT mouse, extravasation appears markedly greater, resulting in almost confluent fluorescence in portions of the ischemic area.

Scale bars: 100 μm.

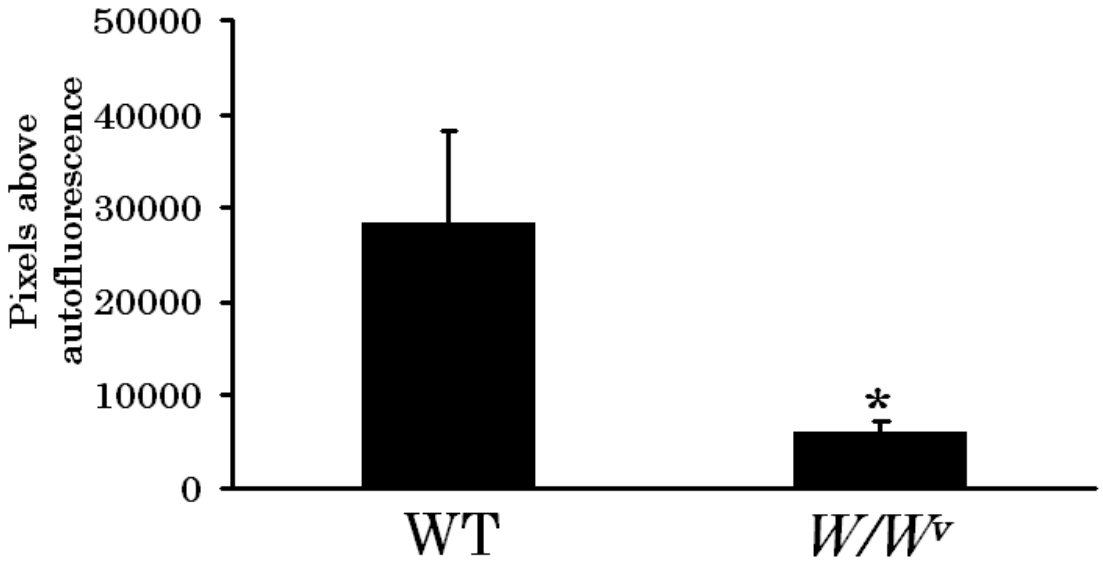

Fig. 3-3.

Evans-blue albumin fluorescent signal representing the magnitude of extravasation and BBB leakage in WT and *W/W^V* mice.

Values are significantly different ($P<0.05$) from WT mice.

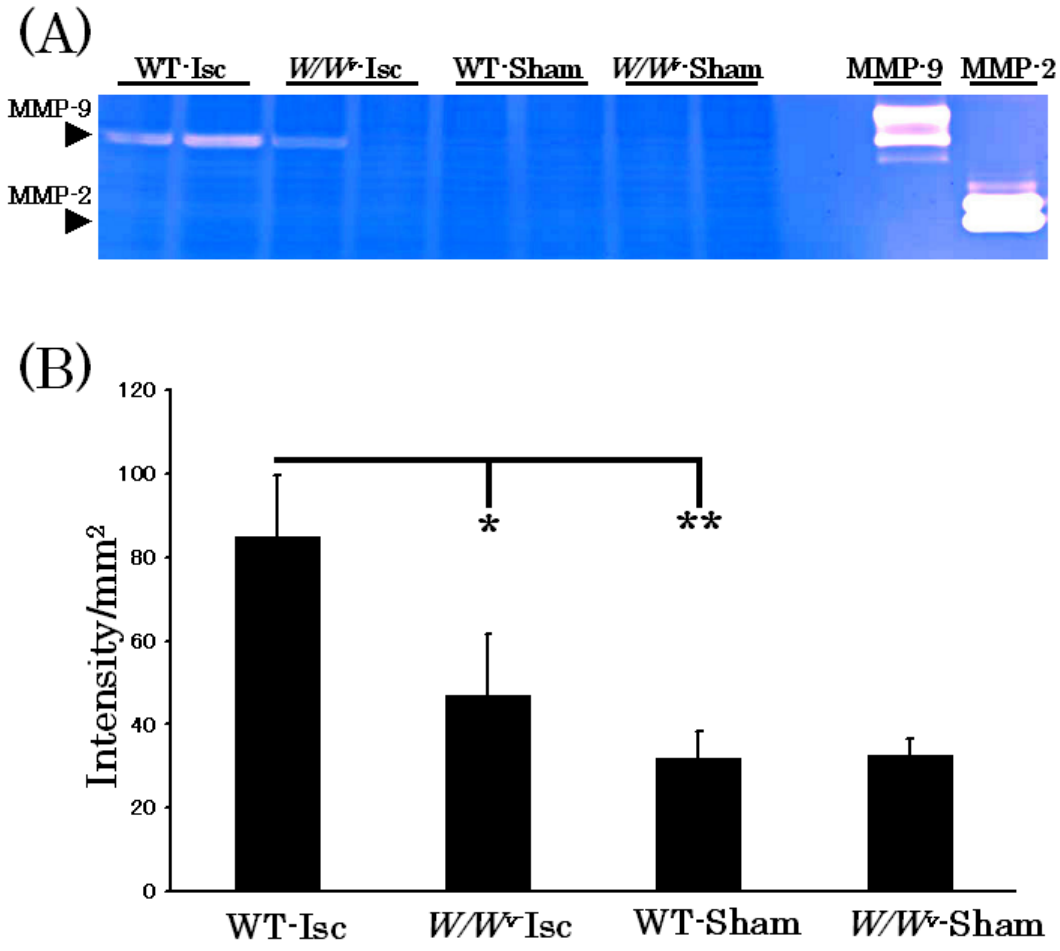

Fig. 3-4

(A) Representative gelatin zymography showing MMP-9 and MMP-2 from the cortex in WT and *W/W^{V}* mice either ischemia-treated or sham-operation treated. The indicative bands represent murine MMP-9 or MMP-2, shown by positive controls (recombinant MMP-9 or MMP-2).

Note that ischemia-treated WT mice showed defined bands of MMP-9, while in ischemia-treated *W/W^{V}* mice MMP-9 were weakly expressed.

(B) Changes in expression of active MMP-9. Values are significantly different; **, ($P<0.01$) in WT-Isc vs. WT-Sham; *, ($P<0.05$) WT-Isc vs. *W/W^{V}*-Isc.

Abbreviations: Isc, ischemia-treated; Sham, sham-operation treated.

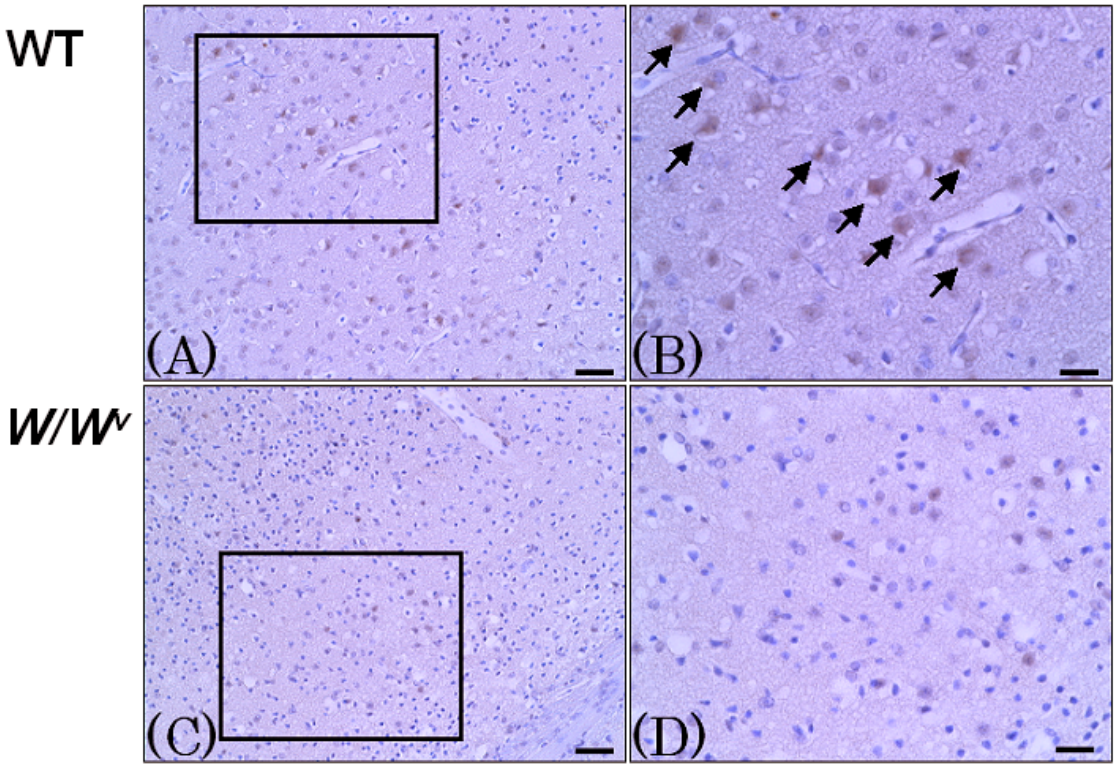

Fig. 3-5

Immunohistological staining with anti-MMP-9 in the cortex from ischemia-treated (A, B) WT, and (C, D) *W/W^{V}* mouse. (A, B) In WT mouse, surviving neurons in the peri-ischemic areas were positive for MMP-9 (arrows). (C, D) *W/W^{V}* mouse had few immunoreacted neurons. (B) and (D) indicate the magnification of windows in (A) and (C), respectively.

Scale bars: (A, C) 50 μm, (B, D) 25 μm.

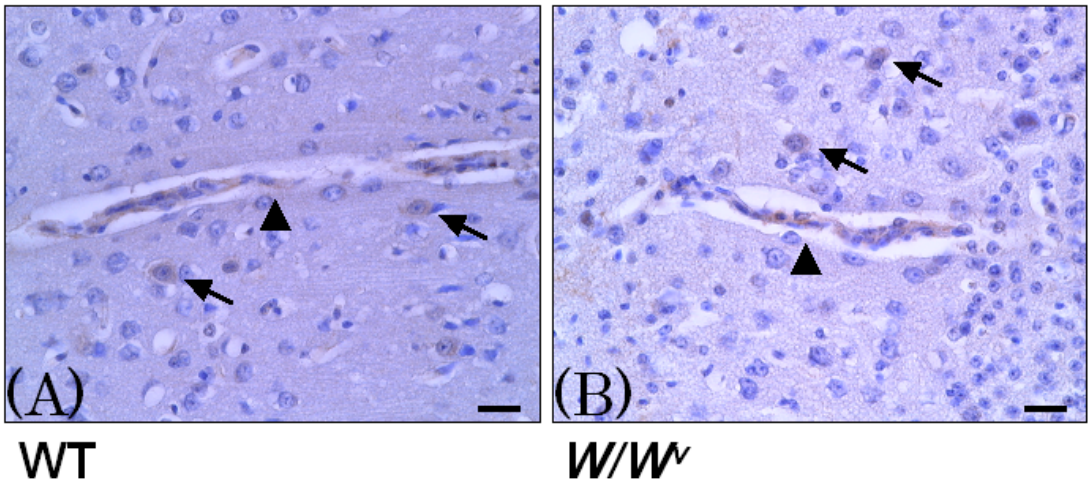

Fig. 3-6

Immunohistological staining with anti-TIMP-1 in the cortex from ischemia-treated (A) WT, and (B) *W/W^{v}* mouse. In both WT and *W/W^{v}* mice, TIMP-1 immunoreaction was diffusely detected in the neurons (arrows) and blood vessel walls (arrowheads).

Scale bars: 25 μm.

General Discussion

In Chapter 1, direct occlusion of the distal MCA was performed in C57BL/6 mice and was characterized by ischemic insults. Direct MCAO method has kept a high survivability of animals and shown high reproducibility of infarct lesions within MCA territory. This method is more adequate than the other methods for the observation of ischemic insults, involving neuronal cell death, glial cell reactions and BBB damage. Furthermore, surgeons can make focal models without regard to variations in arterial augmentation or diameter, which interfere with induction of consistent lesions in the intraluminal thread MCAO model. I conclude that direct MCAO is a very useful method for the induction of focal ischemic lesion in mice.

In Chapter 2 and 3, I studied the roles of mast cell in brain ischemia using murine focal and global ischemic models. Mast cells are stationary cellular mediators of immediate hypersensitivity and show local phlogistic reactions to mechanical, toxic, and allergic stimuli [Grimbaldeston et al., 2006; Bischoff, 2007]. Strbian et al. [2006] reported that pharmacological degranulation of mast cell promoted ischemic BBB permeability and neutrophil infiltration in the early ischemic model. In my study of Chapter 2, both pharmacological mast cell stabilization and absence of mast cell in the gene-manipulated *W/W^v* mice strongly suppressed expansion of focal ischemic lesion from 12 h to 2 day after direct MCAO. It was discussed that formation of initial infarct lesion, which was promoted or inhibited corresponding to mast cell modulations, impacted on subsequent lesion development. Furthermore, I considered one possibility that mast cells also participated in initial activation of macrophages/microglias. At the early ischemic stage, mast cells would have important multi functions to process the edematous and inflammatory mechanisms.

In the case of global ischemic model in Chapter 3, concomitant with the reduction of MMP-9 expression in *W/W^v* mice, both neurological deficits and ischemic areas were limited, and BBB damage was remarkably reduced when compared with those of WT mice. These results indicated that mast cells also participated in pathophysiology of global ischemia, as well as focal ischemia. At 24 h after global ischemia, in zymography analysis active MMP-9 was increased in the brain samples from WT mice, showing immunohistological positive reactions in cortical neurons, glial cells and infiltrated neutrophils. On the other hand, *W/W^v* mice showed the reduction of active MMP-9 expression, suggesting the reflection of decrease in number of MMP-9 positive neurons. It was discussed that in *W/W^v* mice inflammatory stimuli might be weak against neuronal cells by loss of mast cell functions, so that these mice would show the reduction of BBB damage followed MMP-9 production.

From the present studies and previous reports, I considered three functions of mast cell on participation of ischemic process: 1) promotion of BBB permeability through release of many vasoactive agents (TNF-α, histamine, bradykinin, prostaglandins, leukotriens, platelet-activating factor, nitric oxide), 2) BBB damage and tissue breakdown through release of proteolytic enzymes (MMPs, chymase, tryptase), 3) inflammatory stimuli for neurons and macrophages/microglias as well as previously mentioned neutrophils, via proinflammatory cytokines (TNF-α, IL-1) release. These functions are indicated in a schema (Fig. GD-1). The stimulators for mast cell are unclear. However, as well as plasma extravasation in BBB damage and subarachnoid hemorrhage, complement components C3a and C5a are yielded which are the most potent stimulators of mast cell [Lindsberg et al., 1996]. And

adenosine, that dramatically increased under ischemia as consequence of energy metabolism failure, activates mast cells via A_3 adenosine receptor [Ramkumar et al., 1993; Latini and Pedata, 2001; Rossi et al., 2007].

On the other hand, it is reported that mast cells have potentially roles on neuroprotection. Neurotrophic and/or tropic cues (e.g. nerve growth factor) could be produced directly by mast cells [Leon et al., 1994]. And histamine suppresses the ATP depletion during ischemia by preventing energy consumption [Adachi et al., 2005]. Possibly, brain mast cells may have a good function at the chronic stage of brain ischemia. It is, however, necessary for more detailed examinations in the long term.

My studies support the hypothesis that following ischemic stroke brain mast cells are activated and participate in the subsequent pathophysiological process. Mast cells would have roles of BBB permeability and damage, exacerbating edematous formation. And inflammatory stimuli from mast cells might link to neuroinflammation. As a therapeutic treatment, stabilization of brain mast cells could be a new target at the early ischemic stage.

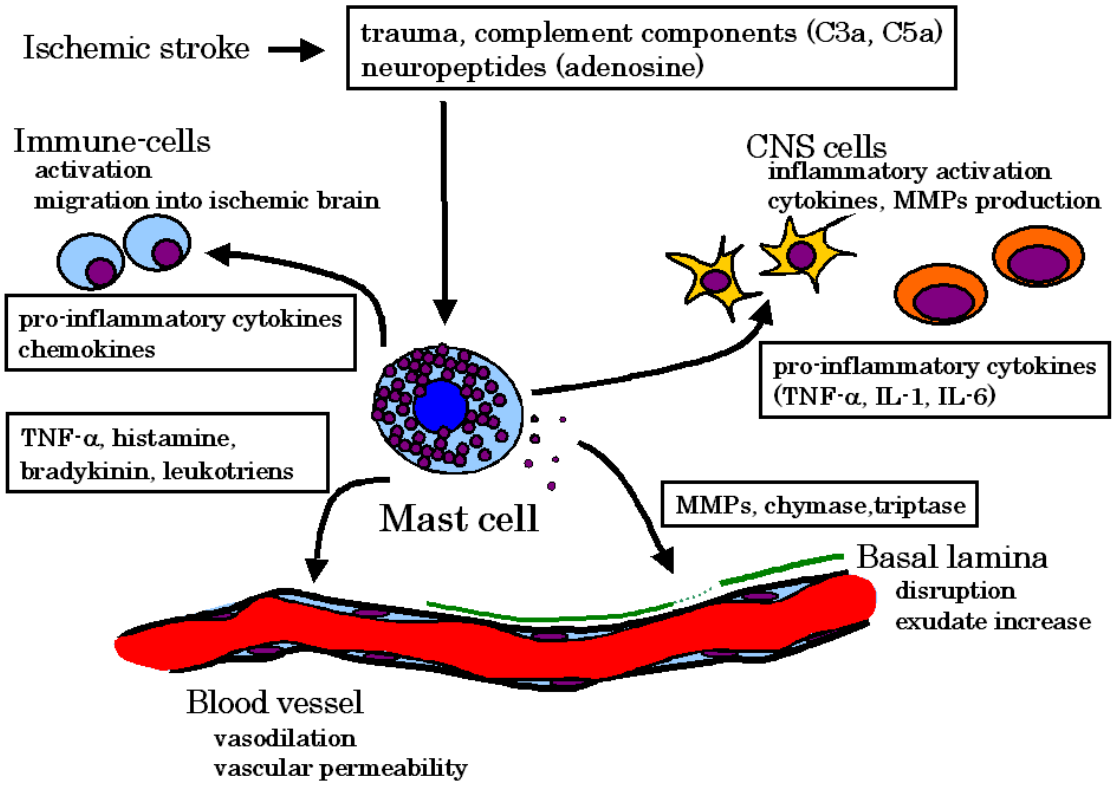

Fig. GD-1

Roles of brain mast cell following ischemic stroke. Mast cells are activated by traumatic and/or molecular stimulators, and promote the edematous and inflammatory mechanisms.

Abbreviations: central nervous system (CNS), matrix metalloproteinases (MMPs), tumor necrosis factor-α (TNF-α), interleukin-1, -6 (IL-1, -6).

Refferences

Adachi, N., 2005. Cerebral ischemia and brain histamine. Brain Res. Brain Res. Rev. 50, 275-286.

Akassoglou, K., Probert, L., Kontogeorgos, G., Kollias, G., 1997. Astrocyte-specific but not neuron-specific transmembrane TNF triggers inflammation and degeneration in the central nervous system of transgenic mice. J. Immunol. 158, 438-445.

Anthony, D.C., Ferguson, B., Matyzak, M.K., Miller, K.M., Esiri, M.M., Perry, V.H., 1997. Differential matrix metalloproteinase expression in cases of multiple sclerosis and stroke. Neuropathol. Appl. Neurobiol. 23, 406-415.

Asahi, M., Wang, X., Mori, T., Sumii, T., Jung, J.C., Moskowitz, M.A., Fini, M.E., Lo, E.H., 2001. Effects of matrix metalloproteinase-9 gene knock-out on the proteolysis of blood-brain barrier and white matter components after cerebral ischemia. J. Neurosci. 21, 7724-7732.

Asahina, M., Yoshiyama, Y., Hattori, T., 2001. Expression of matrix metalloproteinase-9 and urinary-type plasminogen activator in Alzheimer's disease brain. Clin. Neuropathol. 20, 60-63.

Ayata, C., Ropper, A.H., 2002. Ischaemic brain oedema. J. Clin. Neurosci. 9, 113-124.

Barone, F.C., Knudsen, D.J., Nelson, A.H., Feuerstein, G.Z., Willette, R.N., 1993. Mouse strain differences in susceptibility to cerebral ischemia are related to cerebral vascular anatomy. J. Cereb. Blood Flow. Metab. 13, 683-692.

Bederson, J.B., Pitts, L.H., Germano, S.M., Nishimura, M.C., Davis, R.L., Bartkowski, H.M., 1986. Evaluation of 2,3,5-triphenyltetrazolium chloride as a stain for detection and quantification of experimental cerebral infarction in rats. Stroke. 17, 1304-1308.

Belayev, L., Busto, R., Zhao, W., Fernandez, G., Ginsberg, M.D., 1999. Middle cerebral artery occlusion in the mouse by intraluminal suture coated with poly-L-lysine: neurological and histological validation. Brain Res. 833, 181-190.

Biran, V., Cochois, V., Karroubi, A., Arrang, J.M., Charriaut-Marlangue, C., Héron, A., 2008. Stroke induces histamine accumulation and mast cell degranulation in the neonatal rat brain. Brain Pathol. 18, 1-9.

Bischoff, S.C., 2007. Role of mast cells in allergic and non-allergic immune responses: comparison of human and murine data. Nat. Rev. Immunol. 7, 93-104.

Chan, P.H., 1998. The role of transgenic animals in cerebral ischemia. In: Ginsberg, M.D., Bogousslavsky, J. eds. Cerebrovascular Disease: Pathophysiology, Diagnosis, and Management, Vol. 1. Blackwell, Cambridge, MA, USA, pp. 481-488.

Chandler, S., Miller, K.M., Clements, J.M., Lury, J., Corkill, D., Anthony, D.C., Adams, S.E., Gearing, A.J., 1997. Matrix metalloproteinases, tumor necrosis factor and multiple sclerosis: an overview. J. Neuroimmunol. 72, 155-161.

Chen, S.T., Hsu, C.Y., Hogan, E.L., Maricq, H., Balentine, J.D., 1986. A model of focal ischemic stroke in the rat: reproducible extensive cortical infarction. Stroke. 17, 738-743.

Clark, W.M., Lessov, N.S., Dixon, M.P., Eckenstein, F., 1997. Monofilament intraluminal middle cerebral artery occlusion in the mouse. Neurol. Res. 19, 641-648.

Cocchiara, R., Albeggiani, G., Lampiasi, N., Bongiovanni, A., Azzolina, A., Geraci, D., 1999. Histamine and tumor necrosis factor-alpha production from purified rat brain mast cells mediated by substance P. Neuroreport. 10, 575-578.

Cocchiara, R., Bongiovanni, A., Albeggiani, G., Azzolina, A., Geraci, D., 1998. Evidence that brain mast cells can modulate neuroinflammatory responses by tumour necrosis factor-alpha production. Neuroreport. 9, 95-98.

Coyle, P., 1982. Middle cerebral artery occlusion in the young rat. Stroke. 13, 855-859.

Cunningham, L.A., Wetzel, M., Rosenberg, G.A., 2005. Multiple roles for MMPs and TIMPs in cerebral ischemia. Glia. 50, 329-339.

Dirnagl, U., Iadecola, C., Moskowitz, M.A., 1999. Pathobiology of ischaemic stroke: an integrated view. Trends Neurosci. 22, 391-397.

Fang, K.C., Wolters, P.J., Steinhoff, M., Bidgol, A., Blount, J.L., Caughey, G.H., 1999. Mast cell expression of gelatinases A and B is regulated by kit ligand and TGF-beta. J. Immunol. 162, 5528-5535.

Fotheringham, A.P., Davies, C.A., Davies, I., 2000. Oedema and glial cell involvement in the aged mouse brain after permanent focal ischaemia. Neuropathol. Appl. Neurobiol. 26, 412-423.

Frank, B.T., Rossall, J.C., Caughey, G.H., Fang, K.C., 2001. Mast cell tissue inhibitor of metalloproteinase-1 is cleaved and inactivated extracellularly by alpha-chymase. J. Immunol. 166, 2783-2792.

Franklin, K.B.J., Paxinos, G., 1997. The Mouse Brain in Stereotaxic Coordinates. Academic Press, San Diego, CA, USA.

Frosch, M.P., Anthony, D.C., De Girolami, U., 2005. The cerebral nervous system. In: Kumar, V., Abbas, A.D., Fausto, N. eds. Robbins & Cotran Pathologic Basis of Diseases, 7 th ed. Elsevier Sanders, Philadelphia, PA, USA, pp. 1243-1244.

Garden, G.A., Möller, T., 2006. Microglia biology in health and disease. J. Neuroimmune Pharmacol. 1, 127-137.

Gong, C., Qin, Z., Betz, A.L., Liu, X.H., Yang, G.Y., 1998. Cellular localization of tumor necrosis factor alpha following focal cerebral ischemia in mice. Brain Res. 801, 1-8.

Gordon, J.R., Galli, S.J., 1991. Release of both preformed and newly synthesized tumor necrosis factor alpha (TNF-alpha)/cachectin by mouse mast cells stimulated via the Fc epsilon RI. A mechanism for the sustained action of mast cell-derived TNF-alpha during IgE-dependent biological responses. J. Exp. Med. 174, 103-107.

Greene, J., Wang, M., Liu, Y.E., Raymond, L.A., Rosen, C., Shi, Y.E., 1996. Molecular cloning and characterization of human tissue inhibitor of metalloproteinase 4. J. Biol. Chem. 271, 30375-30380.

Grimbaldeston, M.A., Metz, M., Yu, M., Tsai, M., Galli, S.J., 2006. Effector and potential immunoregulatory roles of mast cells in IgE-associated acquired immune responses. Curr. Opin. Immunol. 18, 751-760.

Grzanna, R., Shultz, L.D., 1982. The contribution of mast cells to the histamine content of the central nervous system: a regional analysis. Life Sci. 30, 1959-1964.

Hacke, W., Schwab, S., Horn, M., Spranger, M., De Georgia, M., von Kummer, R., 1996. 'Malignant' middle cerebral artery territory infarction: clinical course and prognostic signs. Arch. Neurol. 53, 309-315.

Hartley, C.J., Reddy, A.K., Madala, S., Entman, M.L., Michael, L.H., Taffet, G.E., 2004. Noninvasive ultrasonic measurement of arterial wall motion in mice. Conf. Proc. IEEE. Eng. Med. Biol. Soc. 5, 3688-3691.

Hatashita, S., Hoff, J.T., 1990. Brain edema and cerebrovascular permeability during cerebral ischemia in rats. Stroke. 21, 582-588.

Heib, V., Becker, M., Taube, C., Stassen, M., 2008. Advances in the understanding of mast cell function. Br. J. Haematol. 142, 683-694.

Heinsius, T., Bogousslavsky, J., Van-Melle, G., 1998. Large infarcts in the middle cerebral artery territory. Etiology and outcome patterns. Neurology. 50, 341-350.

Hendrix, S., Warnke, K., Siebenhaar, F., Peters, E.M., Nitsch, R., Maurer, M., 2006. The majority of brain mast cells in B10.PL mice is present in the hippocampal formation. Neurosci. Lett. 392, 174-177.

Hermann, D.M., Kuroiwa, T., Hata, R., Gillardon, F., Ito, U., Mies, G., 2001. Expression of redox factor-1, p53-activated gene 608 and caspase-3 messenger RNAs following repeated unilateral common carotid artery occlusion in gerbils-relationship to delayed cell injury and secondary failure of energy state. Neuroscience. 102, 779-787.

Holgate, S.T., 2000. The role of mast cells and basophils in inflammation. Clin. Exp. Allergy. 30, Suppl 1, 28-32.

Hu, W., Xu, L., Pan, J., Zheng, X., Chen, Z., 2004. Effect of cerebral ischemia on brain mast cells in rats. Brain Res. 1019, 275-280.

Jin, Y., Silverman, A.J., Vannucci, S.J., 2007. Mast cell stabilization limits hypoxic-ischemic brain damage in the immature rat. Dev. Neurosci. 29, 373-384.

Johnson, D., Krenger, W., 1992. Interactions of mast cells with the nervous system - recent advances. Neurochem. Res. 17, 939-995.

Kakurai, M., Monteforte, R., Suto, H., Tsai, M., Nakae, S., Galli, S.J., 2006. Mast cell-derived tumor necrosis factor can promote nerve fiber elongation in the skin during contact hypersensitivity in mice. Am. J. Pathol. 169, 1713-1721.

Kanemitsu, H., Nakagomi, T., Tamura, A., Tsuchiya, T., Kono, G., Sano, K., 2002. Differences in the extent of primary ischemic damage between middle cerebral artery coagulation and intraluminal occlusion models. J. Cereb. Blood Flow. Metab. 22, 1196-1204.

Kelly, S., McCulloch, J., Horsburgh, K., 2001. Minimal ischemic neuronal damage and HSP70 expression in MF1 strain mice following bilateral common carotid artery occlusion. Brain Res. 914, 185-195.

Kitagawa, K., Matsumoto, M., Handa, N., Fukunaga, R., Ueda, H., Isaka, Y., Kimura, K., Kamada, T., 1989. Prediction of stroke-prone gerbils and their cerebral circulation. Brain Res. 479, 263-269.

Kitagawa, K., Matsumoto, M., Saido, T.C., Ohtsuki, T., Kuwabara, K., Yagita, Y., Mabuchi, T., Yanagihara, T., Hori, M., 1999. Species differences in fodrin proteolysis in the ischemic brain. J. Neurosci. Res. 55, 643-649.

Kitagawa, K., Matsumoto, M., Yang, G., Mabuchi, T., Yagita, Y., Hori, M., Yanagihara, T., 1998. Cerebral ischemia after bilateral carotid artery occlusion and intraluminal suture occlusion in mice: evaluation of the patency of the posterior communicating artery. J. Cereb. Blood Flow. Metab. 18, 570-579.

Kitamura, Y., Go, S., Hatanaka, K., 1978. Decrease of mast cells in W/W^{v} mice and their increase by bone marrow transplantation. Blood. 52, 447-452.

Lambertsen, K.L., Meldgaard, M., Ladeby, R., Finsen, B., 2005. A quantitative study of microglial-macrophage synthesis of tumor necrosis factor during acute and late focal cerebral ischemia in mice. J. Cereb. Blood Flow. Metab. 25, 119-135.

Latini, S., Pedata, F., 2001. Adenosine in the central nervous system: release mechanisms and extracellular concentrations. J. Neurochem. 79, 463-484.

Leon, A., Buriani, A., Dal Toso, R., Fabris, M., Romanello, S., Aloe, L., Levi-Montalcini, R., 1994. Mast cells synthesize, store, and release nerve growth factor. Proc. Natl. Acad. Sci. USA. 91, 3739-3743.

Lindsberg, P., Ohman, J., Lehto, T., Karjalainen-Lindsberg, M., Paetau, A., Wuorimaa, T., Carpen, O., Kaste, M., Meri, S., 1996. Complement activation in the central nervous system following blood-brain barrier damage in man. Ann. Neurol. 40, 587-596.

Lorenzl, S., Albers, D.S., Narr, S., Chirichigno, J., Beal, M.F., 2002. Expression of MMP-2, MMP-9, and MMP-1 and their endogenous counterregulators TIMP-1 and TIMP-2 in postmortem brain tissue of Parkinson's disease. Exp. Neurol. 178, 13-20.

Maeda, K., Hata, R., Bader, M., Walther, T., Hossmann, K.A., 1999. Larger anastomoses in angiotensinogen-knockout mice attenuate early metabolic disturbances after middle cerebral artery occlusion. J. Cereb. Blood Flow. Metab. 19, 1092-1098.

Maeda, K., Hata, R., Hossmann, K.A., 1998. Differences in the cerebrovascular anatomy of C57black/6 and SV129 mice. Neuroreport. 9, 1317-1319.

Magnoni, S., Baker, A., George, S.J., Duncan, W.C., Kerr, L.E., McCulloch, J., Horsburgh, K., 2004. Differential alterations in the expression and activity of matrix metalloproteinases 2 and 9 after transient cerebral ischemia in mice. Neurobiol. Dis. 17, 188-197.

Martin, L.J., Al-Abdulla, N.A., Brambrink, A.M., Kirsch, J.R., Sieber, F.E., Portera-Cailliau, C., 1998. Neurodegeneration in excitotoxicity, global cerebral ischemia, and target deprivation: A perspective on the contributions of apoptosis and necrosis. Brain Res. Bull. 46, 281-309.

Matsumoto, M., Hatakeyama, T., Akai, F., Brengman, J.M., Yanagihara, T., 1988. Prediction of stroke before and after unilateral occlusion of the common carotid artery in gerbils. Stroke. 19, 490-497.

Mayhan, W.G., 2001. Regulation of blood-brain barrier permeability. Microcirculation. 8, 89-104.

McColl, B.W., Carswell, H.V., McCulloch, J., Horsburgh, K., 2004. Extension of cerebral hypoperfusion and ischaemic pathology beyond MCA territory after intraluminal filament occlusion in C57Bl/6J mice. Brain Res. 997, 15-23.

Muramatsu, K., Fukuda, A., Togari, H., Wada, Y., Nishino, H., 1997. Vulnerability to cerebral hypoxic-ischemic insult in neonatal but not in adult rats is in parallel with disruption of the blood-brain barrier. Stroke. 28, 2281-2289.

Murphy, G., Knäuper, V., Cowell, S., Hembry, R., Stanton, H., Butler, G., Freije, J., Pendás, A.M., López-Otín, C., 1999. Evaluation of some newer matrix metalloproteinases. Ann. NY. Acad. Sci. 878, 25-39.

Nakagawa, Y., Fujimoto, N., Matsumoto, K., Cervós-Navarro, J., 1990. Morphological changes in acute cerebral ischemia after occlusion and reperfusion in the rat. Adv. Neurol. 52, 21-27.

National Institute of Neurological Disorders and Stroke *ad Hoc* Committee, 1990. Special report from the National Institute of Neurological Disorders and Stroke. Classification of cerebrovascular disease III. Stroke. 21, 637-676.

Nocka, K., Tan, J.C., Chiu, E., Chu, T.Y., Ray, P., Traktman, P., Besmer, P., 1990. Molecular bases of dominant negative and loss of function mutations at the murine c-kit/white spotting locus: W37, Wv, W41 and W. EMBO. J. 9, 1805-1813.

Ohtaki, H., Dohi, K., Nakamachi, T., Yofu, S., Endo, S., Kudo, Y., Shioda, S., 2005. Evaluation of brain ischemia in mice. Acta. Histochem. Cytochem. 38, 99-106.

Ozdemir, Y.G., Bolay, H., Erdem, E., Dalkara, T., 1999. Occlusion of the MCA by an intraluminal filament may cause disturbances in the hippocampal blood flow due to anomalies of circle of Willis and filament thickness. Brain Res. 822, 260-264.

Pekny, M., Nilsson, M., 2005. Astrocyte activation and reactive gliosis. Glia. 50, 427-434.

Posner, J.D., Gorman, K.M., Woldow, A., 1984. Stroke in the elderly: I. Epidemiology. J. Am. Geriatr. Soc. 32, 95-102.

Qi, X., Hosoi, T., Okuma, Y., Kaneko, M., Nomura, Y., 2004. Sodium 4-phenylbutyrate protects against cerebral ischemic injury. Mol. Pharmacol. 66, 899-908.

Ramkumar, V., Stiles, G.L., Beaven, M.A., Ali, H., 1993. The A3 adenosine receptor is the unique adenosine receptor which facilitates release of allergic mediators in mast cells. J. Biol. Chem. 268, 16887-16890.

Rivera, S., Ogier, C., Jourquin, J., Timsit, S., Szklarczyk, A.W., Miller, K., Gearing, A.J., Kaczmarek, L., Khrestchatisky, M., 2002. Gelatinase B and TIMP-1 are regulated in a cell- and time-dependent manner in association with neuronal death and glial reactivity after global forebrain ischemia. Eur. J. Neurosci. 15, 19-32.

Romanic, A.M., White, R.F., Arleth, A.J., Ohlstein, E.H., Barone, F.C., 1998. Matrix metalloproteinase expression increases after cerebral focal ischemia in rats: inhibition of matrix metalloproteinase-9 reduces infarct size. Stroke. 29, 1020-1030.

Rosenberg, G.A., 1999. Ishemic brain edema. Prog. Cardiovasc. Dis. 42, 209-216.

Rosenberg, G.A., Estrada, E.Y., Dencoff, J.E., 1998. Matrix metalloproteinases and TIMPs are associated with blood-brain barrier opening after reperfusion in rat brain. Stroke. 29, 2189-2195.

Rosenberg, G.A., Estrada, E.Y., Dencoff, J.E., Stetler-Stevenson, W.G., 1995. Tumor necrosis factor-alpha-induced gelatinase B causes delayed opening of the blood-brain barrier: an expanded therapeutic window. Brain Res. 703, 151-155.

Rosenberg, G.A., Cunningham, L.A., Wallace, J., Alexander, S., Estrada, E.Y., Grossetete, M., Razhagi, A., Miller, K., Gearing, A., 2001. Immunohistochemistry of matrix metalloproteinases in reperfusion injury to rat brain: activation of MMP-9 linked to stromelysin-1 and microglia in cell cultures. Brain Res. 893, 104-112.

Rossi, D.J., Brady, J.D., Mohr, C., 2007. Astrocyte metabolism and signaling during brain ischemia. Nat. Neurosci. 10, 1377-1386.

Russell, W.L., Henry, D.P., Phebus, L.A., Clemens, J.A., 1990. Release of histamine in rat hypothalamus and corpus striatum in vivo. Brain Res. 512, 95-101.

Saarinen, J., Kalkkinen, N., Welgus, H.G., Kovanen, P.T., 1994. Activation of human interstitial procollagenase through direct cleavage of the Leu83-Thr84 bond by mast cell chymase. J. Biol. Chem. 269, 18134-18140.

Silver, R., Silverman, A.J., Vitković, L., Lederhendler, I.I., 1996. Mast cells in the brain: evidence and functional significance. Trends Neurosci. 19, 25-31.

Simard, J.M., Kent, T.A., Chen, M., Tarasov, K.V., Gerzanich, V., 2007. Brain oedema in focal ischaemia: molecular pathophysiology and theoretical implications. Lancet. Neurol. 6, 258-268.

Small, D.L., Buchan, A.M., 2000. Animal models. Br. Med. Bull. 56, 307-317.

Small, D.L., Morley, P., Buchan, A.M., 1999. Biology of ischemic cerebral cell death. Prog. Cardiovasc. Dis. 42, 185-207.

Steiner, D.R., Gonzalez, N.C., Wood, J.G., 2003. Mast cells mediate the microvascular inflammatory response to systemic hypoxia. J. Appl. Physiol. 94, 325-334.

Strbian, D., Durukan, A., Pitkonen, M., Marinkovic, I., Tatlisumak, E., Pedrono, E., Abo-Ramadan, U., Tatlisumak, T., 2008. The blood-brain barrier is continuously open for several weeks following transient focal cerebral ischemia. Neuroscience. 153, 175-181.

Strbian, D., Karjalainen-Lindsberg, M.L., Tatlisumak, T., Lindsberg, P.J., 2006. Cerebral mast cells regulate early ischemic brain swelling and neutrophil accumulation. J. Cereb. Blood Flow Metab. 26, 605-612.

Tagaya, M., Haring, H.P., Stuiver, I., Wagner, S., Abumiya, T., Lucero, J., Lee, P., Copeland, B.R., Seiffert, D., del Zoppo, G.J., 2001. Rapid loss of microvascular integrin expression during focal brain ischemia reflects neuron injury. J. Cereb. Blood Flow Metab. 21, 835-846.

Takano, K., Tatlisumak, T., Bergmann, A.G., Gibson, D.G. 3rd, Fisher, M., 1997. Reproducibility and reliability of middle cerebral artery occlusion using a silicone-coated suture (Koizumi) in rats. J. Neurol. Sci. 153, 8-11.

Tamaki, M., Kidoguchi, K., Mizobe, T., Koyama, J., Kondoh, T., Sakurai, T., Kohmura, E., Yokono, K., Umetani, K., 2006. Carotid artery occlusion and collateral circulation in C57Black/6J mice detected by synchrotron radiation microangiography. Kobe J. Med. Sci. 52, 111-118.

Tanuma, N., Sakuma, H., Sasaki, A., Matsumoto, Y., 2006. Chemokine expression by astrocytes plays a role in microglia/macrophage activation and subsequent neurodegeneration in secondary progressive multiple sclerosis. Acta. Neuropathol. 112, 195-204.

Tetlow, L.C., Harper, N., Dunningham, T., Morris, M.A., Bertfield, H., Woolley, D.E., 1998. Effects of induced mast cell activation on prostaglandin E and metalloproteinase production by rheumatoid synovial tissue in vitro. Ann. Rheum. Dis. 57, 25-32.

Theoharides, T.C., 1990. Mast cells: the immune gate to the brain. Life Sci. 46, 607-617.

Thomas, W.E., 1992. Brain macrophages: evaluation of microglia and their functions. Brain Res. Brain Res. Rev. 17, 61-74.

Tsuchiya, D., Hong, S., Kayama, T., Panter, S.S., Weinstein, P.R., 2003. Effect of suture size and carotid clip application upon blood flow and infarct volume after permanent and temporary middle cerebral artery occlusion in mice. Brain Res. 970, 131-139.

Ward, R., Collins, R.L., Tanguay, G., Miceli, D., 1990. A quantitative study of cerebrovascular variation in inbred mice. J. Anat. 173, 87-95.

Warnick, R.E., Fike, J.R., Chan, P.H., Anderson, D.K., Ross, G.Y., Gutin, P.H., 1995. Measurement of vascular permeability in spinal cord using Evans Blue spectrophotometry and correction for turbidity. J. Neurosci. Methods. 58, 167-171.

Wexler, E.J., Peters, E.E., Gonzales, A., Gonzales, M.L., Slee, A.M., Kerr, J.S., 2002. An objective procedure for ischemic area evaluation of the stroke intraluminal thread model in the mouse and rat. J. Neurosci. Methods. 113, 51-58.

Xi, G.M., Wang, H.Q., He, G.H., Huang, C.F., Wei, G.Y., 2004. Evaluation of murine models of permanent focal cerebral ischemia. Chin. Med. J. 117, 389-394.

Yamamoto, M., Tamura, A., Kirino, T., Shimizu, M., Sano, K., 1988. Behavioral changes after focal cerebral ischemia by left middle cerebral artery occlusion in rats. Brain Res. 452, 323-328.

Yang, G., Kitagawa, K., Matsushita, K., Mabuchi, T., Yagita, Y., Yanagihara, T., Matsumoto, M., 1997. C57BL/6 strain is most susceptible to cerebral ischemia following bilateral common carotid occlusion among seven mouse strains: selective neuronal death in the murine transient forebrain ischemia. Brain Res. 752, 209-218.

Zhuang, X., Silverman, A.J., Silver, R., 1996. Brain mast cell degranulation regulates blood-brain barrier. J. Neurobiol. 31, 393-403.

Acknowledgements

The author wishes to express my gratitude to professor Y. Yoshikawa and associate professor S. Kyuwa (Department of Biomedical Science, the University of Tokyo) for supervising this doctorial thesis, and assistant professor T. Furuta (Department of Microbiology and Immunology, The Institute of Medical Science, University of Tokyo) for advising research objective and providing precious samples. Also, the author is deeply grateful to assistant professor Y, Ishii (Department of Biomedical Science, the University of Tokyo) for studious discussions, and to assistant professor T. Matsuwaki for technical advice and backup of my study.

The author would like to thank Ms. Y. Tanishima for careful supports, Ms. M. Kakinuma for enjoying shared interests, and all the members of Department of Biomedical Science. They have continuously given me helpful advice, encouragement, and joyful time throughout the doctorial course.